

Loss of *BAP1* expression is associated with an immunosuppressive microenvironment in uveal melanoma, with implications for immunotherapy development

Carlos R Figueiredo^{1,2*}, Helen Kalirai¹, Joseph J Sacco^{1,3}, Ricardo A Azevedo⁴, Andrew Duckworth¹, Joseph R Slupsky¹, Judy M Coulson⁵ and Sarah E Coupland^{1,6}

¹ Department of Molecular and Clinical Cancer Medicine, ITM, University of Liverpool, Liverpool, UK

² Department of the Faculty of Medicine, MediCity Research Laboratory and Institute of Biomedicine, University of Turku, Turku, Finland

³ Department of Medical Oncology, The Clatterbridge Cancer Centre, Wirral, UK

⁴ Department of Cancer Biology, The University of Texas–MD Anderson Cancer Center, Houston, TX, USA

⁵ Department of Cellular and Molecular Physiology, University of Liverpool, Liverpool, UK

⁶ Liverpool Clinical Laboratories, Royal Liverpool University Hospital, Liverpool, UK

*Correspondence to: CR Figueiredo, MediCity Research Laboratory and Institute of Biomedicine, University of Turku, Tykistökatu 6, 20520 Turku, Finland. E-mail: crdefi@utu.fi

Abstract

Immunotherapy using immune checkpoint inhibitors (ICIs) induces durable responses in many metastatic cancers. Metastatic uveal melanoma (mUM), typically occurring in the liver, is one of the most refractory tumours to ICIs and has dismal outcomes. Monosomy 3 (M3), polysomy 8q, and *BAP1* loss in primary uveal melanoma (pUM) are associated with poor prognoses. The presence of tumour-infiltrating lymphocytes (TILs) within pUM and surrounding mUM – and some evidence of clinical responses to adoptive TIL transfer – strongly suggests that UMs are indeed immunogenic despite their low mutational burden. The mechanisms that suppress TILs in pUM and mUM are unknown. We show that *BAP1* loss is correlated with upregulation of several genes associated with suppressive immune responses, some of which build an immune suppressive axis, including HLA-DR, CD38, and CD74. Further, single-cell analysis of pUM by mass cytometry confirmed the expression of these and other markers revealing important functions of infiltrating immune cells in UM, most being regulatory CD8⁺ T lymphocytes and tumour-associated macrophages (TAMs). Transcriptomic analysis of hepatic mUM revealed similar immune profiles to pUM with *BAP1* loss, including the expression of IDO1. At the protein level, we observed TAMs and TILs entrapped within peritumoural fibrotic areas surrounding mUM, with increased expression of IDO1, PD-L1, and β -catenin (CTNNB1), suggesting tumour-driven immune exclusion and hence the immunotherapy resistance. These findings aid the understanding of how the immune response is organised in *BAP1*⁻ mUM, which will further enable functional validation of detected biomarkers and the development of focused immunotherapeutic approaches.

© 2020 The Authors. *The Journal of Pathology* published by John Wiley & Sons Ltd on behalf of Pathological Society of Great Britain and Ireland.

Keywords: uveal melanoma; immunotherapy resistance; immune profile; NanoString; CyTOF; digital spatial profiling

Received 8 September 2019; Revised 28 December 2019; Accepted 14 January 2020

No conflicts of interest were declared.

Introduction

Uveal melanoma (UM) is the most common primary intraocular cancer in adults, accounting for 5% of all melanomas [1]. Treatment options for primary UM (pUM) include radiotherapy and surgery [2], and usually achieve excellent local tumour control. Despite this, about 50% of UM patients develop metastatic disease, mainly in the liver [1]. The average survival of patients with metastatic UM (mUM) is ~12 months, as there are currently no proven effective treatments [3]. Resection of isolated liver metastases may be attempted in selected cases, otherwise liver-directed therapy (e.g. percutaneous perfusion with

melphalan) or systemic chemotherapy. Recently, following the striking benefits in metastatic skin melanoma, immunotherapy using immune checkpoint inhibitors (ICIs) has been more widely used in cancer. However, in marked contrast to cutaneous melanoma, mUM is almost universally refractory to ICIs, mostly against CTLA-4 and PD1/PDL-1, with responses to single agents in the range of 3–8% [3].

While UMs have been partly ascribed to a low mutational burden [4,5], evidence of specific TCR gene expression in tumour-infiltrating lymphocytes (TILs) [6], promising responses to adoptive cell therapy using TILs [7], and encouraging results on

targeting the melanocyte-specific gp100 with the bispecific molecule tebentafusp (IMCgp100) [8] all suggest a specific immune response and that mutational burden is not the sole reason for the lack of response to ICI.

Monosomy 3 (M3) has long been known to be associated with increased risk of UM metastasis [9–11], and more recently, it has become apparent that this is primarily due to inactivating mutations of the *BAP1* gene, which has been reported to be a stronger prognosticator than M3 [12,13]. The Cancer Genome Atlas (TCGA) study of 80 pUMs demonstrated that patients with pUM at high metastatic risk [i.e. with UM characterised by M3 and loss of function of the tumour suppressor gene *BAP1* (Chr 3p21.1)] could be further stratified, according to the presence of CD8⁺ T-cell immune infiltrates and an altered transcriptional immune profile [4]. The latter included elevated levels of HLA-I molecules, which leads to natural killer (NK) cell suppression [14], TAM markers and expression of immune checkpoint regulators (ICRs), such as PD-L1, indoleamine 2,3-dioxygenase (IDO)-1, and T-cell Ig and ITIM domain (TIGIT) [4,15].

Interestingly, previous work showed that loss of *BAP1* in turn affects the expression of genes that impact the immune response [16]. In this study, a comprehensive immune profiling of the 80 pUMs from the TCGA-UM study revealed that several immune-suppressive genes are significantly upregulated following *BAP1* loss. We provide a novel and comprehensive understanding of UM immune evasion by profiling primary and metastatic UM at the transcriptomic and protein level using cutting-edge approaches, including mass cytometry, NanoString, and digital spatial profiling of human patient tissues. Our findings suggest that UM cells, particularly those of *BAP1*-negative (*BAP1*⁻) UM, shape the immune profile at both primary and metastatic sites, harnessing the expression of particular pathways and molecules to drive regulatory functions of myeloid cells and lymphocytes, and thus immunosuppression and immunotherapy resistance in advanced UM. These findings provide new insight for the functional validation of detected biomarkers for the further development of novel adjuvant immunotherapeutic approaches.

Materials and methods

Human subjects

This work was underpinned by the University of Liverpool (UoL) Ocular Oncology Biobank (OOB) and the Liverpool Bioinnovation Hub Biobank. Project specific approvals for work with pUM and mUM samples were obtained (REC-18/LO/1027). Four fresh enucleated pUMs were included in this study for the CyTOF analyses.

TCGA analysis

mRNA expression and clinical data of The Cancer Genome Atlas (TCGA) GDC Ocular Melanomas dataset

(UVM) were downloaded from the Xena Functional Genomics Explorer of University of California, Santa Cruz (<https://xenabrowser.net/heatmap>) [17]. To provide understanding of the biological pathways involved in pUM pathogenesis via the expression of different immune genes, the nCounter PanCancer Immune Profiling gene set of 730 genes (NanoString Technologies, Seattle, WA, USA) was applied in the UCSC Cancer Genomics Browser to analyse the enrichment of immune genes sorted by *BAP1* mRNA expression or chromosome 3 copy number variations. Generated data were extracted in comma-separated values (CSV) format and analysed in GraphPad Prism 6 (GraphPad Software, Inc, San Diego, CA, USA) for correlation studies. Supervised clustering of immune genes of the TCGA RNA-seq dataset was performed among those with significant Spearman's correlation to *BAP1* expression or chromosome 3 copy number variation and sorted from the lowest rank (negative correlation) to the highest rank (positive correlation). The list of sorted genes was then uploaded in the Xena Browser for generation of heatmaps. Each of these genes was individually analysed as a prognosticator marker in Kaplan–Meier curves at the Xena Browser along the TCGA-UM cohort. Those genes predicting significant survival differences ($p < 0.05$) were selected for further immune network analysis using the nCounter immune category list (NanoString Technologies) complemented by a custom-built leukocyte functional immune response network collated by literature review (supplementary material, Table S1). Network plots were generated using the NodeXL Basic add-in to Excel. In brief, immune genes were assigned to different immune categories in separated columns. In our analysis, we also considered the low- and high-variance state of these genes along the TCGA-UM cohort. This, in part, helped to define our hypothesis that the degree of variation in the expression of the genes associated with a particular network is indicative of the plasticity of that network [18]. Therefore, high variance is associated with increased plasticity (higher thickness of network lines) and low variance with diminished plasticity (lower thickness of network lines) in response to *BAP1* expression changes. We calculated the expression variance (σ^2) of genes across the TCGA-pUM cohort to predict how *BAP1* loss impacts upon the expression of a particular gene by applying the following formula: $\sigma^2 = \Sigma(X - \mu)^2/N$, where X represents the RNA-seq expression value of a particular gene, μ is the mean of the entire RNA expression for this particular gene in the cohort, and N is the distribution number (TCGA-UM, $N = 80$). Therefore, the higher the effect of *BAP1* on the gene expression, the higher the σ^2 value of this particular gene in the cohort. In the network analysis, the highest variance value was limited to 5 units, assuming the *CCL24* gene as reference for the highest variance ($\sigma^2 = 35.7$). Sphere size represents the number of genes assigned to a given immune category (supplementary material, Tables S2 and S3). Box and whiskers analysis of specific genes according with different *BAP1* expression levels was performed. RNA levels of *BAP1* were defined as high ($n = 27$), mid ($n = 26$), or low ($n = 27$)

according to a Kaplan–Meier survival analysis of three groups in the TCGA-UM cohort generated in the Xena Browser for *BAP1* gene expression ($p = 0.004843$ and log-rank test statistic = 10.66).

Immunohistochemistry

FFPE pUM and mUM samples were sectioned at 4 μm thickness and underwent antigen retrieval using the Dako pretreatment module (Agilent Technologies UK Ltd, Stockport, UK); slides were then incubated in a high-pH bath containing Tris/EDTA buffer, pH 9.0 (Dako EnVision™ FLEX, Agilent) at 96°C for 20 min. IHC was performed using a Dako Autostainer PLUS machine, using the Dako Envision™ FLEX Kit (Agilent) according to the manufacturer's instructions. Slides were incubated with the following antibodies for 30 min: BAP1 (cat. No sc-28 383/C-4, dilution 1:200; Santa Cruz Biotechnology, Dallas, TX, USA), CD3 (cat. No IR503/polyclonal, ready to use; Dako Cytomation, CA, USA), CD4 (cat. No NCL-L-CD4/368, dilution 1:20; Leica Biosystems, Lincolnshire, IL, USA), CD8 (cat. No M7103/ C8/144B, dilution 1:200; Dako), CD163 (NCL-L-CD163/10D6, dilution 1:400; Leica Biosystems), and CD38 (NCL-L-CD38-290/SPC32, dilution 1:100; Leica Biosystems).

The sections were counterstained with haematoxylin. Additional sections were treated with isotype controls at the same concentration as the primary antibodies.

Mass cytometry antibodies and reagents

All metal-chelated optimised antibodies and reagents were purchased from Fluidigm (San Francisco, CA, USA). Full information for the antibodies and reagents used are provided in supplementary material, Table S4. The Maxpar Human Immune Monitoring Panel Kit was used as a reference antibody panel to immune profile primary uveal melanoma tumours, which includes the immune markers recommended by the Human Immunophenotyping Consortium (HIPC) [19], with some modifications. The antibodies used cover the phenotype and functions of different subpanels of B cells, T cells, monocytes, dendritic cells, and NK cells. The MaxPar Panel Designer browser (Fluidigm) was used to predict and avoid metal spillover among tagged metals of the following additional markers included in the customised panel: CD74, LAG-3, CD56, CD16, CTLA-4, CD11b, and CD62L. The following markers were removed from the panel design in order to avoid spillover: CD194, TCR $\gamma\delta$, CD185, CD45RO, CD24, CD197, and CD20. Final spillover results were considered low between channels and this is shown in supplementary material, Figure S1A, top. The final wheel-heatmap of the customised antibody panel shows the function that determines the best antibody–tag combinations to minimise background among channels, which ultimately contains targets with low tolerance of signal overlap (yellow-green).

Mass cytometry of pUM

Four fresh histopathologically-phenotyped BAP1[−] pUMs were manually minced prior to enzymatic digestion using collagenase A (cat. No C9722, 2 mg/ml; Sigma Aldrich, St Louis, MO, USA) and 40 units/ml DNase-I (cat. No 79254; Qiagen, Germantown, MD, USA) in DMEM and incubated with agitation at 37°C for 60 min in a thermal mixer (Thermo Fisher, Waltham, MA, USA). Following incubation, digests were passed through a 70 μm filter to remove residual particulates. Cells were then pelleted (centrifugation at 1500 rpm for 5 min), washed in PBS, and viable cells were quantified using a Trypan Blue exclusion viability dye. Live cells were then washed twice with ice-cold cell staining buffer (ic-CSB; Fluidigm) and total cell concentration was determined using a Neubauer chamber. Up to three staining reactions of a maximum of 2.0×10^6 cells per sample were analysed. All samples were then incubated with 50 μl of 2% mouse serum in PBS with human TruStain FcX solution (Biolegend, San Diego, CA, USA) at 4 °C for 15 min. Samples were then processed for surface and intracellular staining with the panel described in supplementary material, Table S4 using the following protocol: 50 μl of a 2X surface antibody solution was made in ic-CSB (final antibody dilution 1:100) and left on ice for 30 min. Cells were washed and fixed in 5 mM BS3 (Sigma) for 30 min, followed by fixation using 1x Fix-I buffer according to the manufacturer's protocol (Fluidigm), and permeabilised in ice-cold methanol for 10 min. Cells were washed and incubated with internal antibody cocktail (final dilution 1:100) for 30 min in ice. Then cells were washed and resuspended in intercalator-Ir at 1:8000, and processed to be analysed using a Helios mass cytometer (Fluidigm).

Analysis of human tumour mass cytometry datasets

Data from mass cytometry were normalised to the EQ 4-element bead signal using normalisation software version 2 (Fluidigm). Live Ir⁺CD45⁺ cells were manually gated as previously described [20] (supplementary material, Figure S1A, bottom), and FCS files were downloaded for concatenated analysis using Cytosplore V.2.2.1 for further downstream analysis by hierarchical stochastic neighbour embedding (HSNE) using a coefficient of 4 [21], or individually processed for visualisation of t-distributed stochastic neighbour embedding (tSNE) analysis in Cytobank. For accurate clustering and frequency calculations, a cut-off of 1000 events was considered for the final gate. Eventually, Ir^{hi} CD45⁺ tumour infiltrated cells are detected among singlets and exhibit specific TAM markers, but not lymphocytic markers, excluding the possibility of doublets. These cells may often carry tumour-derived DNA and melanin content given to phagocytosed tumour cells and are often observed in primary uveal melanoma tumours, classified as melanophages [22].

Mass cytometry and NanoString data (transcriptomic and DSP data) have been deposited at Flow Cytometry data.

<https://flowrepository.org/id/FR-FCM-Z2FD> and GEO (gene datasets, GSE145782).

mRNA expression analysis using NanoString technology

For RNA immune gene expression analysis, four pUMs, six mUMs, and one normal liver (NL) formalin-fixed, paraffin-embedded (FFPE) samples were used. Only the tumour areas were selected for RNA extraction, or the entire normal liver tissue. The RNeasy FFPE Kit (Qiagen) was used for tissue dissociation, RNA extraction, and purification according to the manufacturer's instructions (Qiagen), as described in supplementary material, Supplementary materials and methods.

The NanoString nSolver 2.6 software was used for normalisation of expression counts using housekeeping genes following the manufacturer's recommendations [23]. Data are displayed in expression count units of individual gene per patient compared with normal liver tissue, and internally normalised within each immune category (e.g. CTL suppression, M2 macrophage regulation, and immune checkpoint regulators). A full range of immune categories is displayed in supplementary material, Table S1.

Digital spatial profiling of mUM tissues

Digital spatial profiling analysis of one BAP1⁻ mUM case was performed by NanoString's DSP technology platform to enable digital characterisation of protein distributed on the surface of FFPE tissue sections using the Human Immune Oncology panel (NanoString Technologies). In brief, 4- to 6- μ m-thick FFPE mUM sections were stained for lymphocytes (CD3, red), macrophages (CD68, magenta), S100B (green), and DNA (blue) in order to detect the regions of interest (ROIs). The following workflow was used: deparaffinisation of FFPE unstained sections, antigen retrieval, antibody staining, ROI selection, DSP technology processing, nCounter analysis system. Data analysis and quality control were processed and normalised using positive and negative anti-mouse and anti-rabbit hybridisation control antibodies. S6 ribosomal protein and histone 3 were used as reference proteins. Area normalisation was applied between different ROI sizes varying from 100 to 650 μ m in diameter. Results are displayed as absolute expression counts normalised with negative IgG controls.

Quantification and statistical analysis

All data were analysed using GraphPad Prism 6.0 and are presented as the means \pm SD. Significant differences in the immune gene expression between the BAP1^{lo}, BAP1^{mid}, and BAP1^{hi} groups were estimated using one-way analysis of variance followed by Bonferroni's multiple comparisons test. Survival analysis was performed in the Xena Browser using the Kaplan–Meier assay and was compared using the log-rank test. The correlation between different mRNA expressions and overall survivals (OS) of TCGA-UM patients was evaluated by non-parametric Spearman's correlation, two-tailed,

where $*0.01 < p < 0.05$, $**0.001 < p < 0.01$; $***0.0001 < p < 0.001$, and $****p < 0.0001$ were considered to indicate significant differences.

Results

BAP1 loss significantly correlates with the modulation of immune genes and patient survival in UM

In the previous TCGA-UM analysis, Robertson *et al* reported that the M3 phenotype in UM is associated with the upregulation of 30 immune genes [4,24], and we therefore first sought to investigate whether this association could be the result of BAP1 loss. We found that an absence or reduced expression of BAP1 mRNA (cut-off 19.54 for BAP1 expression and 2500 days as the default end-point) also significantly correlated with decreased survival, similar to M3 status (cut-off -0.3649 for Chr3 copy number and 2500 days as the default end-point) (Figure 1A). Using Spearman's correlation analysis, we demonstrate that most of the investigated immune genes have a better expression correlation with BAP1 mRNA loss than with M3 (Figure 1B). In addition, only about 50% of these genes are significantly associated with patient survival, indicated by blue squares representative of Kaplan–Meier statistical test results (Figure 1B and supplementary material, Table S5).

We further expanded this analysis by interrogating the TCGA-UM RNA-seq data with a panel of 730 immune genes defined by the nCounter PanCancer immune panel (NanoString Technologies). One hundred and forty-two immune genes exclusively correlated with BAP1 expression, but not with chromosome 3 copy number variation (supplementary material, Table S6); the expression of 117 genes negatively and another 25 genes positively correlated with BAP1 expression (r scores varying from -0.53 to 0.46). Among 181 immune genes that significantly correlated with both BAP1 expression and chromosome 3 copy number variation, 151 genes were negatively correlated and 30 genes were positively correlated, all with a higher correlation score to BAP1 expression than to chromosome 3 (r scores varying from -0.60 to 0.67) (supplementary material, Table S7). Among BAP1 correlated genes ($n = 323$), 168 genes that were negatively correlated with BAP1 expression were significantly associated with decreased survival, while 15 genes positively correlated with BAP1 expression were significantly associated with improved survival (Figure 1C and supplementary material, Table S8).

Independent of BAP1 expression, the M3-UM genotype exclusively correlates with 43 immune genes and with 82 immune genes that also correlate with BAP1 to a lower degree (supplementary material, Tables S9 and S10), from which 48 are upregulated immune genes and 17 are downregulated immune genes, all significantly associated with patient survival (Figure 1C and supplementary material, Table S11). Supervised clustering analysis based on BAP1 mRNA expression is shown,

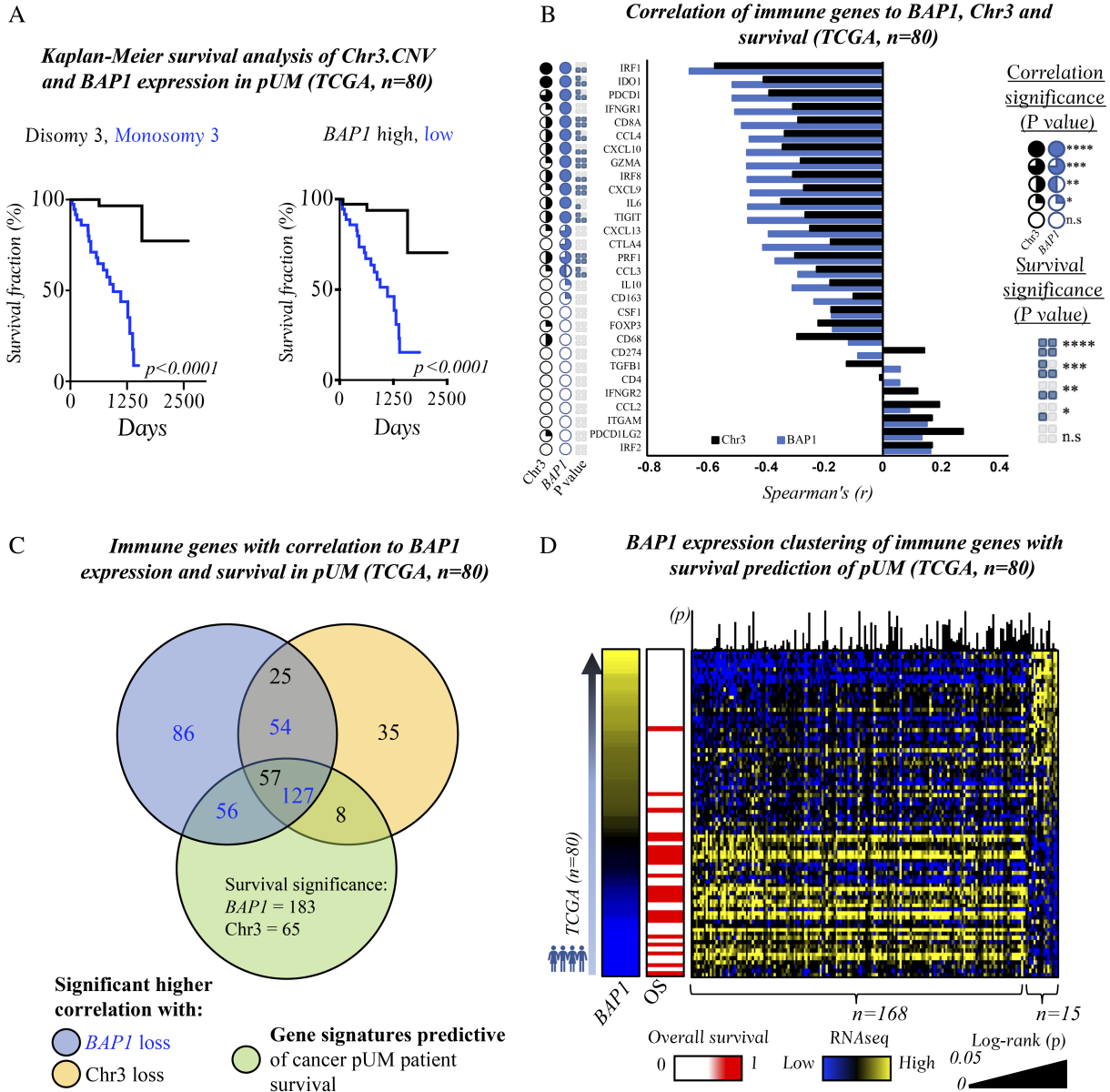


Figure 1. *BAP1* loss significantly correlates with the modulation of immune genes and patient survival in pUM. (A) Decreased mRNA expression of *BAP1* is significantly correlated with a poor survival of primary UM patients similarly to the monosomy 3 (M3) status in the TCGA cohort. (B) Spearman's correlation analysis of specific immune genes compared to *BAP1* expression and to chromosome 3 (Chr3) copy number variation. (C) Venn diagram depicting immune genes with significant correlation to Chr3 and *BAP1* and with predictive survival significance. (D) Heatmap cluster analysis sorted by *BAP1* expression showing upregulated and downregulated immune genes, including the *P*value profile of Kaplan–Meier survival scores.

including the *P* value profile of each gene related to survival outcome (Figure 1D). These findings suggest that loss of *BAP1* expression is strongly associated with immune modulation of the microenvironment in pUM.

***BAP1* loss correlates with immunosuppressive networks in pUM**

We next analysed the group of immune genes upregulated following *BAP1* loss, to predict the likely effects on the microenvironment. A scatter plot shows the gene expression and variance of 168 upregulated immune genes following *BAP1* loss along the TCGA-UM cohort,

highlighting important immune genes involved in immune-suppressive pathways, including *LGALS3*, *CD74*, *CD38*, *PDCD1*, *IDO1*, and *HLA-DR* (Figure 2A). Differential expression analysis revealed that most of these immune genes are significantly upregulated in the TCGA-UM cohort following *BAP1* loss, as shown in the second quadrant of the volcano plot (Figure 2B and supplementary material, Table S8). *PDCD1* and *IDO1* have high significance with $-\log P$ values higher than 1.5 and \log_2FC lower than 0.2, and for that reason are not visible in the volcano plot.

Importantly, all *BAP1* significantly correlated immune genes simultaneously integrate different subcategories of

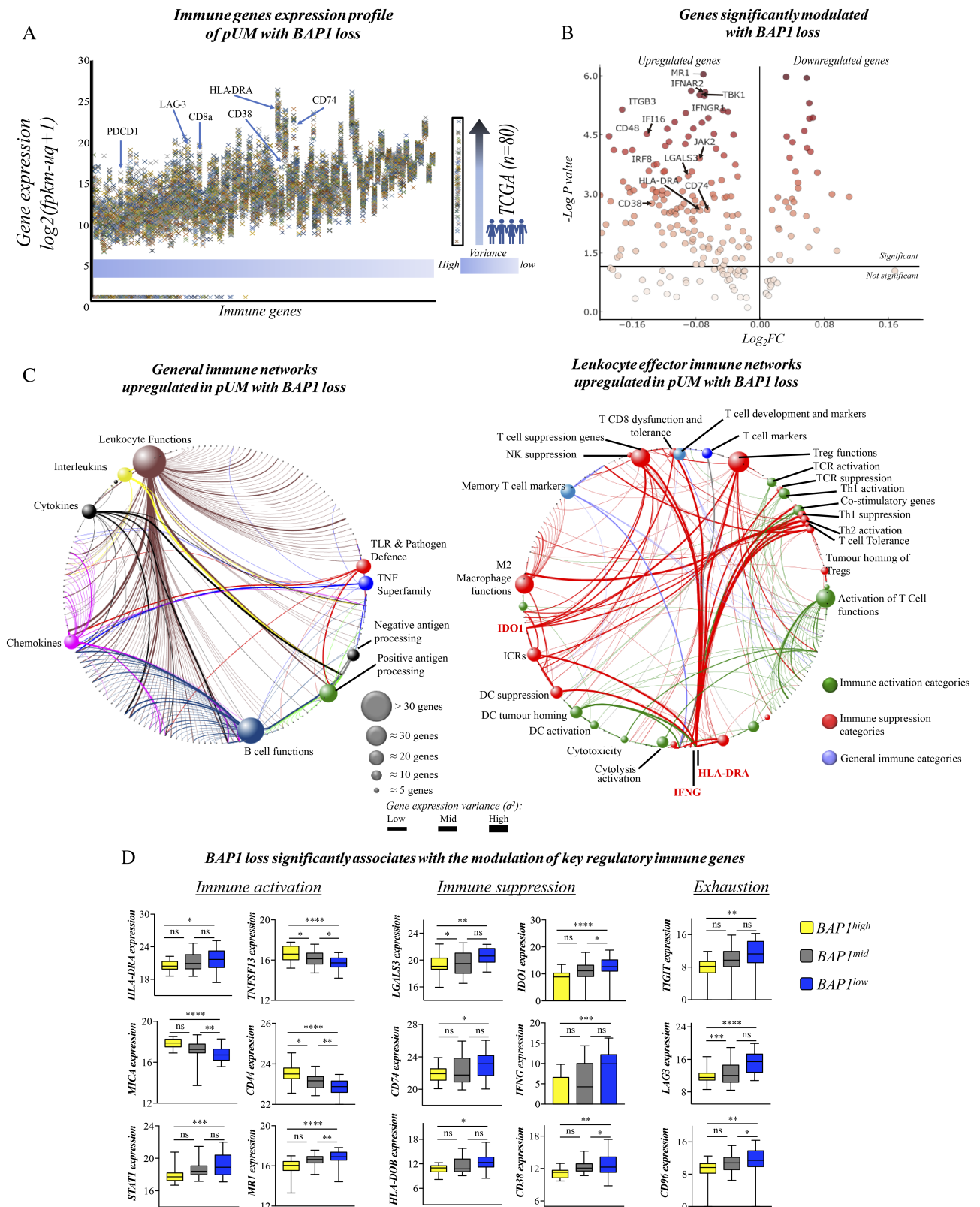


Figure 2. BAP1 loss correlates with increased regulatory immune networks in primary uveal melanoma. (A) Gene expression profile of the TCGA-UM cohort (n = 80) sorted from genes with the highest (left) to the lowest (right) gene variance expression. (B) Volcano plot depicting the most significantly upregulated immune genes with BAP1 loss (black arrows), which have potential immunosuppressive functions. (C) Immune network subcategory integrations with upregulated genes following BAP1 loss. The left panel shows general immune response networks and the right panel shows an expanded leukocyte effector immune response network. (D) Box and whiskers plots of selected upregulated and downregulated immune genes according to BAP1 expression levels (high, mid, and low). One-way ANOVA was used for statistical analysis with Bonferroni's multiple comparisons test. ****p < 0.00001, ***p < 0.0001, **p < 0.001, *p < 0.05.

the immune response, which were used to build an interactive transcriptomic network for visualisation of the predominant immune profile driven by pUM with *BAP1* loss. Therefore, we performed a gene network analysis using two classification systems: a general immune response network based on major immune categories, and an amplified leukocyte functional immune network. In this analysis, the variance of gene expression (σ^2) is represented by the thickness of the network lines, indicating the plasticity of the network toward *BAP1* loss.

This analysis demonstrated that most of modulated immune genes correlate with leukocyte functions, and some of them with chemokine, interleukin, and cytokine expression; B-cell functions; TLR and TNF superfamilies; and antigen presentation processes (Figure 2C). Within the leukocyte network, a dominance of immune-suppressive pathways was observed, represented by red lines predominantly with higher expression variance (higher thickness), including Treg functions, Th1 suppression, Th2 activation, T-cell tolerance responses, homing of Tregs, M2 macrophage functions, and ICRs (Figure 2C). Immune networks related to effective anti-tumour immune responses are represented by green lines, predominantly with lower expression variance (lower thickness).

Importantly, some of the few immune genes that are downregulated following *BAP1* loss (*MICA*, *TNFSF13*, and *CD44*) are important for the activation of anti-tumour immune responses [25–27], as shown in box and whisker plots together with other immunosuppressive and exhaustion-related genes (i.e. *HLA-DOB*, *CD74*, *CD38*, *LGALS3*, *IDO1*, *TIGIT*, *LAG3*, and *CD96*) (Figure 2D). Although HLA-DR has been classified as an immune response activation gene in disease given its importance in peptide presentation to CD4⁺ T cells [28], many regulatory functions have been attributed to HLA-DR expression in the context of cancer [29]. For that reason, in the network analysis, HLA-DR was classified as immunosuppressive, although the generic immune activation classification was kept in Figure 2D. Immune genes that have a significant correlation with M3 status but do not correlate with *BAP1* expression are probably regulated by different mechanisms that exclude *BAP1* involvement. Among these genes, those related with immune response activation are downregulated, including *IL12RB12*, *TLR1*, and *TLR5*, and those involved with suppression of immune response are upregulated, including *FN1*, *CD70*, and *CD73* (*NTFE*) (supplementary material, Figure S2A,B). All together, these findings show how different immune genes may integrate similar immune-suppressive categories in high-risk *BAP1*⁻ pUM, suggesting an importance in regulating the immune profile of mUM.

Transcriptomic analysis of mUM reveals a similar gene expression profile to *BAP1*⁻ pUM

In order to compare the transcriptomic immune profiles of the primary and metastatic sites of UM, we performed a NanoString assay interrogating the expression profile

of the nCounter PanCancer Immune Profiling panel using four pUMs and six mUMs, all lacking nuclear *BAP1* expression. Unsupervised cluster analysis was performed revealing a high correlation between most pUM and mUM cases, with the exception of one mUM (mUM-06). No significant correlation was observed between a normal liver control and tumour tissues (Figure 3A).

Spearman's correlation test of the total gene expression counts revealed significant similarity between the gene expression of both primary and metastatic groups ($r = 0.92$, $p < 0.0001$) for *BAP1* correlated immune genes (supplementary material, Table S8) (Figure 3B, left). A similar correlation score was also observed for one patient with matched primary and metastatic samples (Figure 3B, middle). Importantly, because the expression of samples of the same cancer generated using the same methodology and normalisation are often very similar, we also evaluated the correlation between our NanoString dataset (normalised counts) and the different samples of the TCGA-UM cohort by applying the same genes. We observed that the normalised RNA-seq data from the TCGA-UM cohort are still highly correlative with the NanoString data, for both the primary and the metastatic tumours (Figure 3B, right).

Strikingly, when comparing the gene expression of six mUM patients with that of one human disease-free liver normal biopsy (normal liver, NL), most mUM patients displayed upregulation of specific immune genes related to suppression of cytolytic T cells (CTLs) (Figure 3C), including HLA-DRA, LGALS3, and CD38 partially [30–38]; ICRs such as *TIM-3* (*HAVCR2*), *HMGB1*, *IDO1*, *LAG3*, and *CD73* (*NT5E*) [39–44]; and TAM functional markers, such as *ANXA1*, *CD74*, *CD9*, *INFAR2*, *MIF*, *PLA2G6*, and *CD163* [36,45,46]. In addition, transcript levels of *NOS2*, a predominant M1 macrophage marker [47], were similar to the levels found in normal liver without tumours. We also found high expression levels of *CD74* and the macrophage migration inhibitory factor (*MIF*) across mUM tissues compared with normal liver. RNA levels of *CD38* were increased compared with the levels found in normal liver. At the protein level, we found that *CD38* was also positively expressed among regions of T-cell infiltrates in one *BAP1*⁻ mUM case, as evidenced by IHC staining (supplementary material, Figure S3H). B cells are nearly absent (low numbers of CD20⁺ cells) in mUM, and cytolytic effector cells seem to be at low activation states, given a paucity of TIA1⁺ cells among the TILs.

These findings suggest that the immune profile of *BAP1*⁻ pUM is similar to mUM at the transcriptome level, suggesting an important role of CTL suppressive molecules, including HLA-DRA and CD38, and TAM-related pathways, where the CD74/MIF axis seems to play an important role driving the M2-like phenotype and potential local tolerogenic responses. Therefore, some of these markers were further evaluated at the protein level of *BAP1*⁻ pUM.

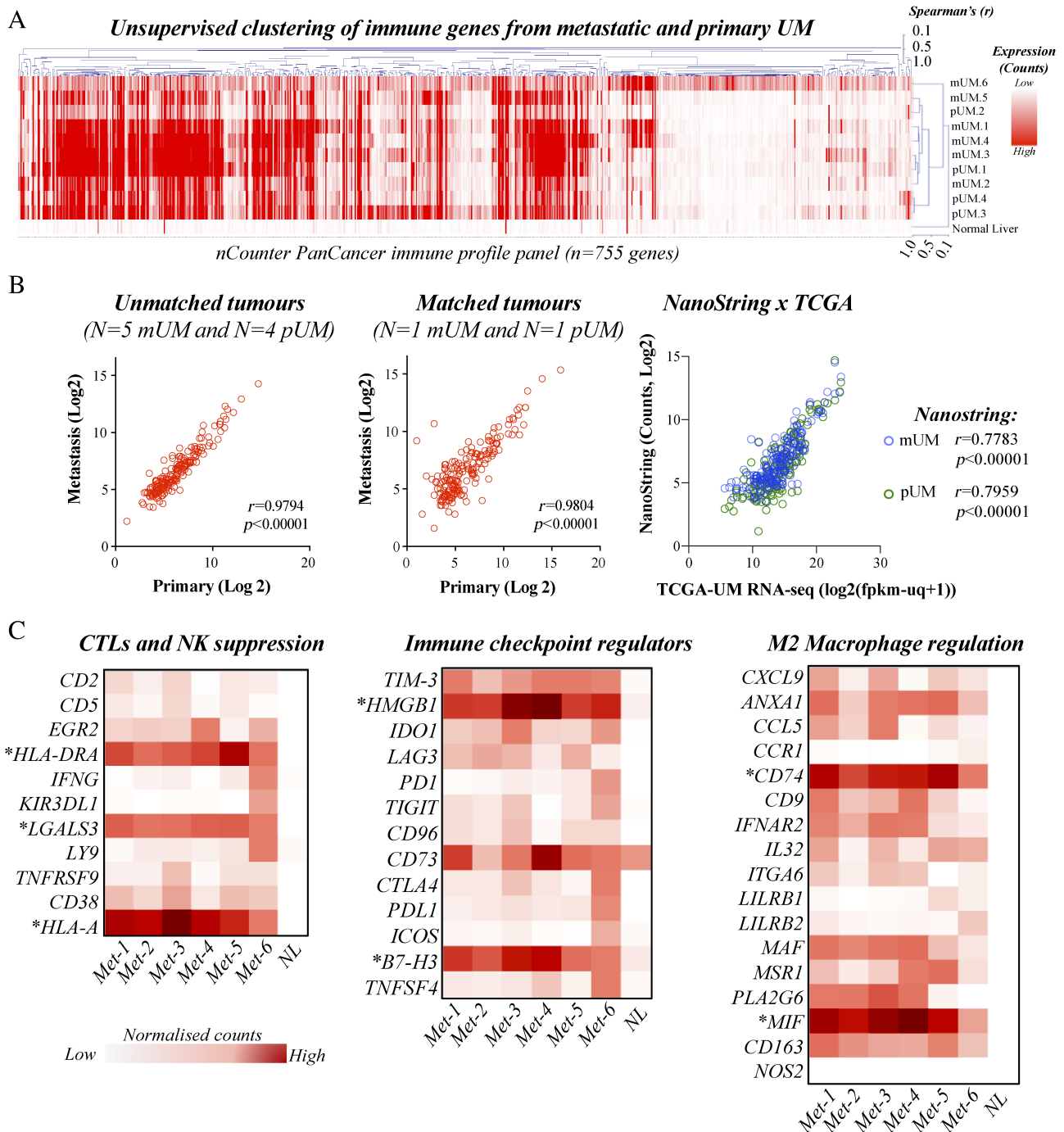


Figure 3. Transcriptomic analysis of *BAP1*-negative metastatic uveal melanoma reveals similar immune profiles to *BAP1*-negative primary tumours. (A) Heatmap of unsupervised clustering of all the samples [mUM ($n = 6$), pUM tissues ($n = 4$), and one normal liver] and all the transcripts (nCounter 730 immune genes panel). (B) Spearman's correlation analysis of gene expression between unmatched tumours from four pUMs and five mUMs (left), two matched tumours from one UM patient using Spearman's correlation rank ($r = 0.92$, $p < 0.0001$) (middle), and pUM/mUM NanoString data correlation analysis with TCGA-UM Fpkm- $uq + 1$ normalised RNA-seq data (right). (C) Heatmap views of normalised RNA expression counts from six mUMs and one normal liver depicting the expression profile of CTL/NK suppression markers, immune checkpoint regulatory markers, and M2 macrophage regulation markers. Asterisks highlight selected highly expressed immune genes across the tissues.

High-resolution single-cell analysis reveals regulatory T-cell phenotype and a mixed macrophage phenotype within pUM with nuclear BAP loss

In order to phenotypically and functionally characterise pUM at the protein level, we performed a high-resolution single-cell analysis using mass cytometry in

five pUMs, four of which showed nuclear *BAP1* loss and one with normal nuclear *BAP1* expression. Among infiltrating $CD45^+$ cells, we observed a predominant cluster of macrophages, T lymphocytes ($CD8^+$ and $CD4^+$ T cells), B cells, and DCs, as evidenced in HSNE plots of all samples clustered together (Figure 4A,B).

The frequency of each cell subtype was calculated for samples. The breakdown of the CD45⁺ infiltrating immune cells in BAP1⁻ samples was as follows: CD4⁺ T cells (12%), CD8⁺ T cells (37%), DCs (10%), macrophages (30%), and B cells (11%) (Figure 4C, left). For one BAP1⁺ case, the breakdown of the CD45⁺ infiltrating immune cells was as follows: CD4⁺ T cells (14%), CD8⁺ T cells (59%), DCs (3%), macrophages (22%), and B cells (2%) (Figure 4C, right).

High-dimensional HSNE single-cell frequency clustering analysis and t-SNE analysis (BAP1⁻ cases) were performed among CD45⁺ cells for pUM cases in order to detect major clusters among the different cell subtypes (Figure 4D,E and supplementary material, Figure S1B–D). Across the T-lymphocyte compartment, we observed high expression levels of CD28 receptor on both CD4⁺ (cluster A) and CD8⁺ T cells (clusters B and C), with low expression of CTLA-4 and LAG-3 checkpoint inhibitors (Figure 4D,E, and supplementary material, Figure S1D). Two out of four patients have low CD28 expression in CD8⁺ T-cell clusters (supplementary material, Figure S1D), but no conclusions can be made, given the low number of tumours investigated. However, the frequency of CD28⁺CD8⁺ cells is still lower than CD28⁺CD4⁺ T cells in all four cases examined. CD4⁺ T cells mostly express CD25 and CD127 markers (cluster A, 5.1%), suggesting that they have a T-regulatory phenotype [48–52]. In addition, CD8⁺ T cells were positive for the proliferation marker Ki67 (clusters B–D), which had low expression among CD4⁺ T cells (cluster A) (Figure 4D). The high levels of Ki67 can be partially explained by the greater frequency of proliferating CD8⁺ T cells compared to CD4⁺ T cells. Cluster C (CD38⁺HLA-DR⁺CD8⁺ T cells) is the most frequent CD8⁺ T-cell cluster among BAP1⁻ tumours (13.5%) and also showed increased expression of CD74 (Figure 4D,E).

In accordance with this suppressive phenotype, most CD8⁺CD28⁺ T cells (clusters B–D) were HLA-DR⁺, a phenotype typical of regulatory CD8⁺ T cells [28]. Importantly, CD8⁺ T-cell clusters express high levels of CD38, recently reported to drive regulatory functions on CD8⁺ T cells [38,53]. Although B cells are not predominant in pUM, they could be divided into three subclusters: CD25⁺CD11b⁺ (cluster H), CD25^{low}CD11b⁺ (cluster I), and CD25⁻CD11b⁻CD74⁺ B cells (cluster J) (Figure 4D,E). Interestingly, cluster H showed increased expression of the LAG-3 immune checkpoint regulator. In the macrophage and dendritic cell compartment (MOs and DCs), we found a mixed phenotype of M2-like CD68⁺CD163⁺CD74⁺ macrophages (cluster E, 7.7%), M1-like CD68⁺CD163⁻CD74⁻CD11c⁺CD11b⁺ macrophages (cluster F, 9.7%), and myeloid CD68⁻CD11b⁺CD11c⁺ dendritic cells (cluster G, 7.8%).

No significant differences were observed in the subclusters analysed in the pUM BAP1⁺ sample for the different immune cell subtypes compared with the BAP1⁻ cases, apart from the CD8⁺ T-cell compartment, which showed reduced levels of regulatory CD38⁺HLA-DR^{high}CD8⁺ T-cell cluster (cluster N, 19.9%) compared

with BAP1⁻ tumours, and positive levels of the functional clusters CD38⁻HLA-DR^{low}Ki67⁺CD8⁺ T cells (cluster K 30.8%) and CD38⁻HLA-DR^{low}Ki67⁻CD8⁺ T cells (cluster M, 4.9%) and exhausted CTLA-4⁺HLA-DR^{low}CD8⁺ T cells (cluster L, 3.4%) (supplementary material, Figure S1B,C).

Taken together, we describe the regulatory nature of TILs in UM with nuclear BAP1 loss, particularly CD4⁺ and CD8⁺ T cells, and a mixed macrophage phenotype where M2-like macrophages express higher levels of CD74.

Immune profile of mUM in regions of interaction between macrophages and lymphocytes

A digital spatial profiling assay (DSP, NanoString) revealed the protein expression profile of 31 immune markers in different regions of interest where macrophages (CD68) and lymphocytes (CD3) localised simultaneously in two mUM cases with nuclear BAP1 loss. Co-localisation of macrophages and lymphocytes occurred both within and at the edge of the tumours (Figure 5A). Among the cancer-related markers, we observed the expression of β 2M, STAT3, STING, and β -catenin (Figure 5B). The expression of β 2M suggests that tumour antigens are presented via HLA-A in these tumour areas, thus supporting the efficacy of ICI [54]. Total levels of STAT3 were elevated, but not in its activated phosphorylated form (pY705), which regulates gene transcription for modulation of immunosuppressive factors [55]. The expression of STING suggests a macrophage-mediated hepatic inflammation and fibrogenic process [56].

Importantly, high levels of β -catenin were detected in both mUM patients, which is related to tumour-induced immune exclusion mechanisms [57–59], suggesting an accessory mechanism by which tumours modulate infiltration and proliferation of lymphocytes in the metastatic site.

Among the immune phenotyping markers, we observed discrete, but positive, levels of CD163; high levels of CD68, HLA-DR, and CD11c, and all macrophage and dendritic cell markers; and intermediate levels of the immune checkpoint PD-L1 (Figure 5B). The neutrophil marker CD66b was not detected in the selected ROIs, suggesting that neutrophils are not involved at least in the crosstalk between macrophages and T cells in these particular BAP1⁻ mUM cases. Lymphoid markers CD8A and CD4 were also found to be highly expressed. CD56 levels are relatively low compared with negative controls, suggesting absence of NK cells in the selected regions. However, T regulatory cells seem to be absent as intracellular levels of Foxp3 were not detected among these patients using this technique.

In addition, low positive levels of granzyme B were detected, together with high expression of B7-H3, a checkpoint regulator of lymphocyte functions [60]. We also observed the expression of IDO-1, TIGIT, and VISTA (Figure 5B). IDO-1 is known to induce adaptive resistance to anti-PD1 and anti-CTLA4 immunotherapies [61,62]. In addition, IDO and TIGIT were recently

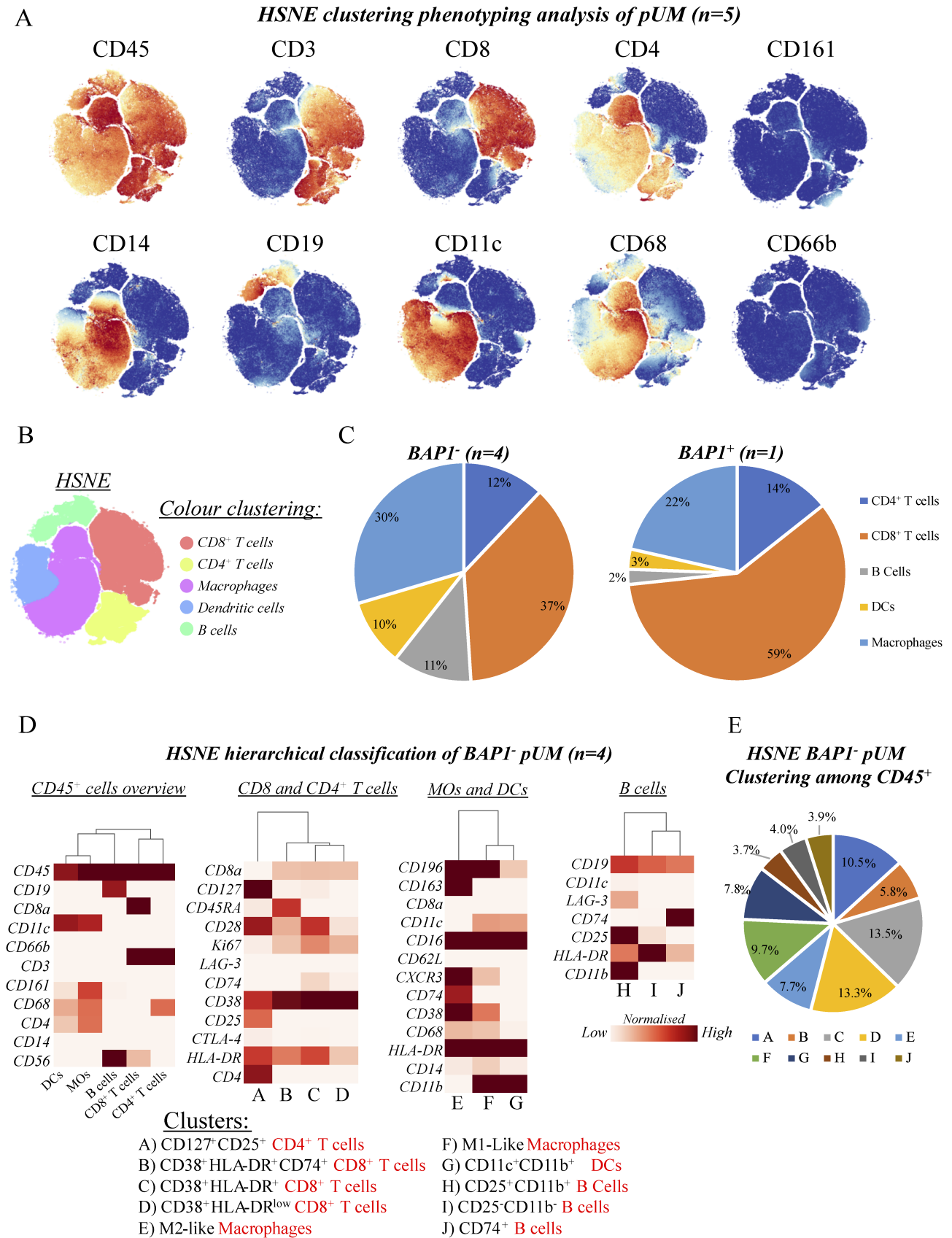


Figure 4. Mass cytometry analysis of infiltrated immune cells in primary UM. (A) Hierarchical stochastic neighbour embedding (HSNE) analysis showing the density of CD45⁺ infiltrated immune cells and selected phenotyping markers of concatenated pUM patients (BAP1⁻, n = 4 and BAP1⁺, n = 1). (B) Colour HSNE maps representing the phenotype of infiltrated immune cell subclusters. (C) Pie frequency charts of infiltrated immune cell subtypes detected by HSNE analysis for BAP1⁻ and BAP1⁺ tumours. (D) Heatmap displaying normalised marker expression of each immune cell cluster for four concatenated BAP1⁻ pUM samples. Analysis was generated in *Cytosplore* highlighting the most frequent clusters of CD45⁺ infiltrated immune cells, and an expanded analysis among tumour infiltrated monocytes, T lymphocytes, and B cells. (E) Pie chart showing the frequency of each cluster identified in HSNE analysis across the four merged BAP1⁻ pUM tumours.

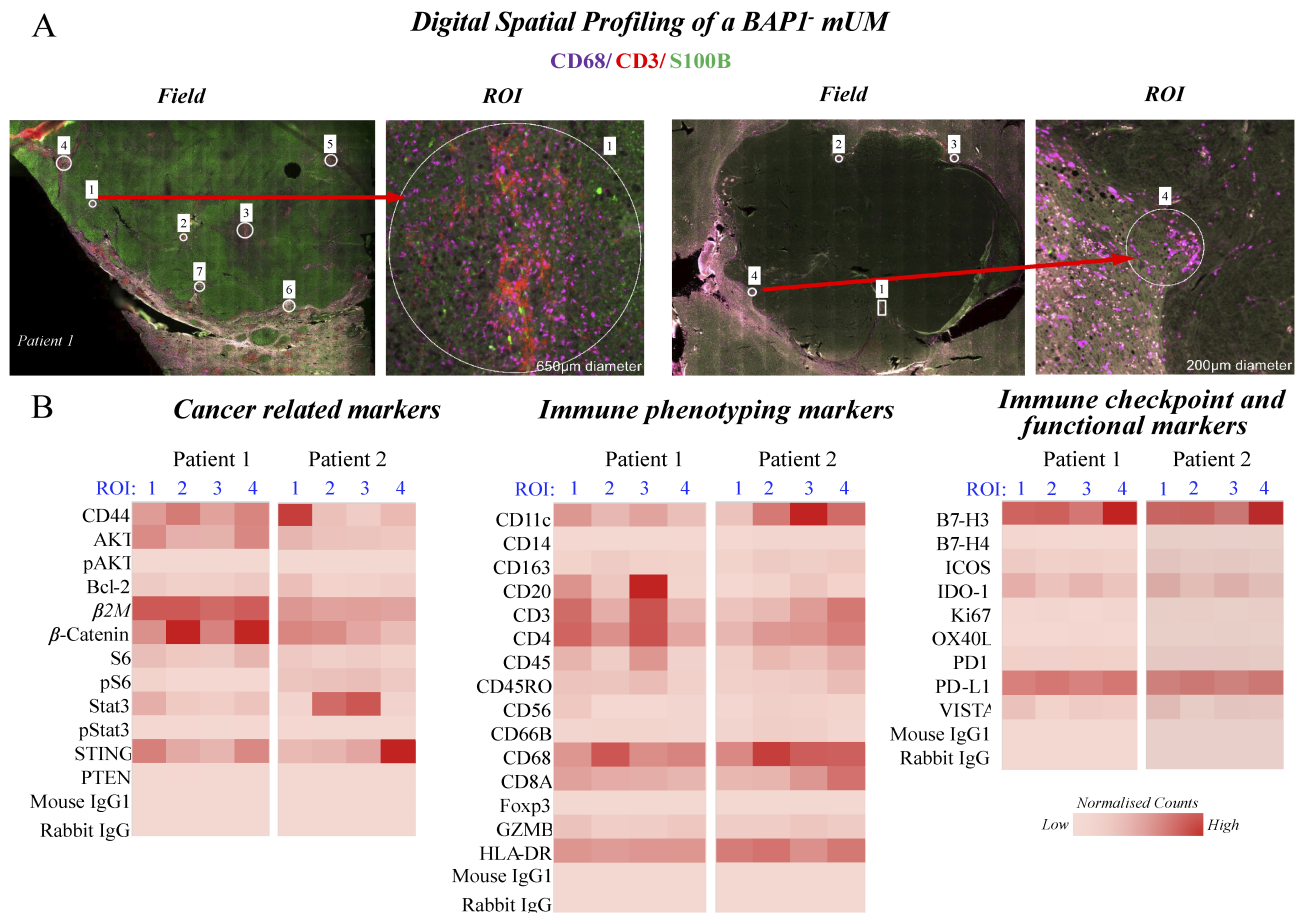


Figure 5. Digital spatial profiling analysis of two mUM BAP1-negative FFPE tissues using the NanoString immune oncology protein panel. (A) Regions of interest (ROI) to evaluate fibrotic areas with high infiltration of both macrophages (CD68) and lymphocytes (CD3). (B) Heatmap representation of different cancer-related markers, immune phenotyping markers, and immune checkpoint and functional markers, all at the protein level among individual ROIs using normalised raw NanoString counts.

described to be expressed in pUM-M3 with corresponding mUM tissues [63].

Considered altogether, these findings suggest alternative mechanisms of T-cell exhaustion other than PD-1 and CTLA-4 engagement, as well as the involvement of mechanisms for immune exclusion that may undertake an important role to support tumour immune evasion and, consequently, immunotherapy failure.

Discussion

In this multi-parametric immunophenotyping work in UM, we profiled the immune response of the 80 patients of the TCGA-UM study, highlighting the involvement of BAP1 loss in the coordination of gene expression of several immune markers. Selected biomarkers were further investigated in a smaller number of primary and metastatic BAP1⁻ UMs, at both transcriptome and protein levels, using cutting-edge techniques. Recently, our group observed that different patterns of nuclear BAP1 expression in pUM provide insights into the prognostic significance of this tumour [64]. Among UMs with an M3 status, the cumulative survival of patients with UM expressing nuclear BAP1 is significantly

greater than that of UM patients whose tumours are M3 with nuclear BAP1 loss. These findings and previous reports associating BAP1 loss with a wide spectrum of cancers [65] underpin the molecular mechanisms behind the adverse prognostic effects of M3, supporting the importance of analysing immune gene expression from the aspect of BAP1 loss in UM.

The genetic diversity of UM was recently described, including copy number variations (CNVs), somatic mutations, and BAP1 alterations [63]. However, the diversity of immune gene expression is described by the tumour stroma (i.e. the features of the reactive cells in the tumour microenvironment), which shapes accordingly with the tumour phenotype (e.g. BAP1 loss). As a consequence of BAP1 loss in UM, tumour cells could therefore unleash metabolic mechanisms to secrete different factors that would induce the regulatory phenotype of T cells and macrophages in the tumour microenvironment (TME) to a more tolerogenic profile. The positive expression of MIF observed at the transcriptomic level in mUM is in accordance with previous reports showing that UM cells can secrete MIF as a mechanism of immune escape [66]. The main receptor of MIF in different immune cells is CD74 [36,67]. In addition, MIF was recently reported to induce M2 polarisation of TAMs, leading to immune suppression on

several solid cancers [34,36,66,68–72], and to downregulate the CTL responses [34], which may occur via its interaction with the CD74 receptor expressed on CD8⁺ T cells in UM, as observed for cluster C. Since CD74 expression was not observed in the CD8⁺ T-cell clusters of one BAP1⁺ pUM, we hypothesise that tumours with reduced expression of MIF or its receptor CD74 may contribute to increase the frequency of more effective CD8⁺ T cells in the TME of UM.

Therefore, modulation of T lymphocytes and macrophages toward an immunosuppressive phenotype could be explained by the expression of CD74 on these cells, which can be affected by suppressive factors derived from tumour cells, including MIF. CD74, which was highly expressed at the transcriptomic level in pUM, was also found at the protein level across the regulatory CD8⁺ T-cell cluster and CD163⁺ M2-like macrophage cluster. CD74 is a chaperone involved in the trafficking of HLA-DR molecules to the surface of immune cells, and while it remains expressed on the surface of the cells, it may bind to MIF secreted by tumour cells in the TME [46,67,73].

The pharmacological blockade of the MIF/CD74 interaction restores the TME immunogenic profile, as well as an effective anti-tumour immune response against metastatic melanoma and gliomas [36,46]. The CD74 monoclonal blocking antibody milatuzumab is currently approved by the Food and Drug Administration (FDA) in the United States for the treatment of multiple myeloma, non-Hodgkin lymphomas, and other CD74⁺ cancers [74,75].

Changes in *BAP1* expression have also been associated with immune transformation in mesothelioma, and became a predictive tool for immunotherapy of peritoneal mesothelioma [76,77]. The impaired ability of thymic development and the proliferative responses of T lymphocytes in the context of *BAP1* inhibition are strong evidence that loss of *BAP1* function is associated with immune suppression and systemic myeloid transformation [16,78].

In this study, we also observed that increased transcriptome levels of CD38, HLA-DRA, IDO1, and LAG-3 are significantly correlated with *BAP1* loss. These immune biomarkers are of extreme importance because they have been associated with different immune-suppressive pathways, which suggests mechanistic insights for immune suppression and immunotherapy resistance using ICIs [30,36–38,41]. In the protein single-cell level, we show the functional state of UM infiltrating CD8⁺ T cells, which co-express high levels of CD38, HLA-DR, and CD28. The co-expression of HLA-DR/CD28 in CD8⁺ T cells suggests that these lymphocytes are distinct from cytolytic effector T cells [30], and can be classified as regulatory CD8⁺ T cells, with similar functions to classical CD4⁺Foxp3⁺ cells [28]. In addition, higher levels of CD38 demarcates regulatory and memory status to CD8⁺ T cells in the context of IFN- γ -mediated immunosuppression, and was recently addressed to drive mechanisms of tumour-mediated immune escape to immunotherapies using PD1/PD-L1

blockade [37,38]. Indeed, IFN- γ is upregulated in the context of *BAP1* loss and is widely associated with several immune-suppressive network categories, which is in accordance with recent reports showing the immune-suppressive roles of IFN- γ [79]. Therefore, targeting CD38 in UM may be considered a suitable strategy to improve the efficacy of immunotherapy using ICI in metastatic UM. A recent study showed that targeting CD38 using isatuximab can preferentially block immunosuppressive T-regulatory lymphocytes and therefore restore immune effector function against multiple myeloma [53].

The low expression of ICRs LAG-3 and CTLA-4 among the majority of T-cell clusters suggests that these lymphocytes may not be exhausted but exist in a lower activation state in pUM [80–83]. Increased transcriptome levels of LAG-3 in the TCGA-UM study could be linked with LAG-3 expression among CD25⁺ B-cell clusters as evidenced by mass cytometry, suggesting a memory and natural regulatory phenotype for these cells [84,85]. Moreover, higher expression of IDO1 in both pUM and mUM suggests this molecule as an important adjuvant target for immunotherapy using ICIs, since IDO1 blockade has been shown to synergise the therapeutic effector of both CTLA-4 and PD1/PD-L1 inhibitors [61].

Our findings in this report also provide evidence that *BAP1*⁻ pUM could shape an immune response similar to that in mUM tissues, since *BAP1*-loss-correlated immune genes are similarly expressed in mUM, as observed using the NanoString approach. Furthermore, the DSP approach revealed that additional ICI-resistant mechanisms not necessarily related to *BAP1* changes may also be important in mUM-induced exclusion of immune cells, such as the Wnt/ β -catenin axis [58,59]. A recent study showed that hepatocellular carcinoma patients displaying an altered Wnt/ β -catenin pathway were refractory to immune-checkpoint blockade [86], which is aligned with evidence that melanoma-intrinsic β -catenin signalling prevents anti-tumour immunity [87].

It is important to highlight that a weakness of this study is the low number of analysed *BAP1*⁻ UM samples for CyTOF studies. The reason behind that is the scarcity of the type of fresh tumour sample, not only because this type of tumour is very rare but also because the tissues must be sufficiently large to provide significant amounts of immune infiltrated cells for further downstream analysis, and thus reducing the sample size of this study. Despite this, we could not only reproduce and confirm previous data published regarding the higher frequency of infiltrated CD8⁺ T cells over CD4⁺ T cells at the transcriptomic and protein levels [4,15], but also detect the expression of specific immune markers initially detected in the transcriptome analysis of the larger TCGA-UM cohort ($n = 80$), and also observed in mUM tissues, expanding the impact of our pUM mass cytometry findings.

The present work shows an improved overview of the immune profile of pUM and mUM at both transcriptome and protein levels and suggests that immune modulation in UM may be driven by loss of *BAP1* expression. Immunosuppressive networks found in *BAP1*⁻ tumours

may not only influence the quality and quantity of local anti-tumour immune responses but also affect immunotherapy outcomes using ICIs, leading to regulation or exclusion of T effector lymphocytes, as well as alternative polarisation of macrophages toward a tolerogenic phenotype in the TME. The relative importance of these findings will require further functional validation, and this study provides the solid ground to initiate these studies. Detected key immune biomarkers, such as CD38 and CD74, could be immediately investigated for functional validation in the adjuvant settings of ICI immunotherapies, since there are currently available FDA-approved inhibitors against these targets [53,74]. Altogether, this work provides the most critical immune markers and pathways to consolidate the type of immune responses in the context of *BAP1* loss in UM. This may help us to understand why this type of cancer is one of the most refractory to current immunotherapies using ICIs at present.

Acknowledgements

The authors Prof Sarah E. Coupland and Dr Helen Kalirai are part of the UMCure2020 consortium. We would like to thank the “Eye Tumour Research Fund” of the Charitable Funds, Royal Liverpool University Hospital, Liverpool, UK, the “Liverpool Ocular Oncology Research Group” (<http://www.loorg.org>), and the North West Cancer Research Centre (NWCRC) for funding this research. Thanks are due to Professor Christiane Hertz-Fowler and Dr Lucille Rainbow from the Centre of Genomic Research (CGR) at the UoL for providing support with NanoString experiments, and to Dr Eva Caamano Gutierrez from the Computational Biology Facility at the UoL for providing initial genomic data analysis support. Thanks are also due to Mohammed Jawad from the University of Liverpool and Dr Christopher Law and Dr Sandra Pereira Cachinho from the Cell Sorting and Mass Cytometry facilities for their support with the mass cytometry work, and to Mr Simon Bidolph, Senior Biomedical Scientist at the Liverpool Clinical Laboratories, for the provision of histological sections for the immunohistochemistry undertaken.

Author contributions statement

CRF performed the research and drafted the manuscript. HK assisted with methodology design, sample collection and preparation, conceptual advice, and manuscript drafting. JJS assisted with methodology design, conceptual advice, and manuscript drafting. RAA assisted with data analysis. AD provided support with mass cytometry data analysis and interpretation of results. SJR provided support to mass cytometry work. JMC assisted with conceptual advice and manuscript drafting. SEC was involved in methodology design and sample collection, supervised the research, and drafted the manuscript.

References

1. Singh AD, Bergman L, Seregard S. Uveal melanoma: epidemiologic aspects. *Ophthalmol Clin North Am* 2005; **18**: 75–84 viii.
2. Kaliki S, Shields CL. Uveal melanoma: relatively rare but deadly cancer. *Eye (Lond)* 2017; **31**: 241–257.
3. Komatsubara KM, Carvajal RD. Immunotherapy for the treatment of uveal melanoma: current status and emerging therapies. *Curr Oncol Rep* 2017; **19**:45.
4. Robertson AG, Shih J, Yau C, et al. Integrative analysis identifies four molecular and clinical subsets in uveal melanoma. *Cancer Cell* 2017; **32**: 204–220.e215.
5. Yarchoan M, Hopkins A, Jaffee EM. Tumor mutational burden and response rate to PD-1 inhibition. *N Engl J Med* 2017; **377**: 2500–2501.
6. Nitta T, Oksenberg JR, Rao NA, et al. Predominant expression of T cell receptor V alpha 7 in tumor-infiltrating lymphocytes of uveal melanoma. *Science* 1990; **249**: 672–674.
7. Chandran SS, Somerville RPT, Yang JC, et al. Treatment of metastatic uveal melanoma with adoptive transfer of tumour-infiltrating lymphocytes: a single-centre, two-stage, single-arm, phase 2 study. *Lancet Oncol* 2017; **18**: 792–802.
8. Sacco JJ, Kalirai H, Kenyani J, et al. Recent breakthroughs in metastatic uveal melanoma: a cause for optimism? *Future Oncol* 2018; **14**: 1335–1338.
9. Coupland SE, Lake SL, Zeschnigk M, et al. Molecular pathology of uveal melanoma. *Eye (Lond)* 2013; **27**: 230–242.
10. Damato B, Coupland SE. Translating uveal melanoma cytogenetics into clinical care. *Arch Ophthalmol* 2009; **127**: 423–429.
11. Angi M, Kalirai H, Prendergast S, et al. In-depth proteomic profiling of the uveal melanoma secretome. *Oncotarget* 2016; **7**: 49623–49635.
12. Jama N, Farquhar N, Butt Z, et al. Altered nuclear expression of the deubiquitylase BAP1 cannot be used as a prognostic marker for canine melanoma. *J Comp Pathol* 2018; **162**: 50–58.
13. Harbour JW, Onken MD, Roberson ED, et al. Frequent mutation of *BAP1* in metastasizing uveal melanomas. *Science* 2010; **330**: 1410–1413.
14. Jager MJ, Hurks HM, Levitskaya J, et al. HLA expression in uveal melanoma: there is no rule without some exception. *Hum Immunol* 2002; **63**: 444–451.
15. Bronkhorst IH, Vu TH, Jordanova ES, et al. Different subsets of tumor-infiltrating lymphocytes correlate with macrophage influx and monosomy 3 in uveal melanoma. *Invest Ophthalmol Vis Sci* 2012; **53**: 5370–5378.
16. Dey A, Seshasayee D, Noubade R, et al. Loss of the tumor suppressor BAP1 causes myeloid transformation. *Science* 2012; **337**: 1541–1546.
17. Cline MS, Craft B, Swatloski T, et al. Exploring TCGA Pan-Cancer data at the UCSC Cancer Genomics Browser. *Sci Rep* 2013; **3**: 2652.
18. Raser JM, O’Shea EK. Noise in gene expression: origins, consequences, and control. *Science* 2005; **309**: 2010–2013.
19. Maecker HT, McCoy JP, Nussenblatt R. Standardizing immunophenotyping for the Human Immunology Project. *Nat Rev Immunol* 2012; **12**: 191–200.
20. Chevrier S, Levine JH, Zanotelli VRT, et al. An immune atlas of clear cell renal cell carcinoma. *Cell* 2017; **169**: 736–749.e718.
21. van Unen V, Höllt T, Pezzotti N, et al. Visual analysis of mass cytometry data by hierarchical stochastic neighbour embedding reveals rare cell types. *Nat Commun* 2017; **8**:1740.
22. Pawelek JM. Viewing malignant melanoma cells as macrophage-tumor hybrids. *Cell Adh Migr* 2007; **1**: 2–6.
23. Danaher P, Warren S, Dennis L, et al. Gene expression markers of tumor infiltrating leukocytes. *J Immunother Cancer* 2017; **5**: 18.

24. Robertson AG, Shih J, Yau C, *et al.* Integrative analysis identifies four molecular and clinical subsets in uveal melanoma. *Cancer Cell* 2018; **33**: 151.
25. Mrass P, Kinjyo I, Ng LG, *et al.* CD44 mediates successful interstitial navigation by killer T cells and enables efficient antitumor immunity. *Immunity* 2008; **29**: 971–985.
26. Chen M, Lin X, Liu Y, *et al.* The function of BAFF on T helper cells in autoimmunity. *Cytokine Growth Factor Rev* 2014; **25**: 301–305.
27. Campbell AR, Duggan MC, Suarez-Kelly LP, *et al.* MICA-expressing monocytes enhance natural killer cell Fc receptor-mediated antitumor functions. *Cancer Immunol Res* 2017; **5**: 778–789.
28. Machicote A, Belén S, Baz P, *et al.* Human CD8. *Front Immunol* 2018; **9**: 2788.
29. Liu X, Zhan Z, Li D, *et al.* Intracellular MHC class II molecules promote TLR-triggered innate immune responses by maintaining activation of the kinase Btk. *Nat Immunol* 2011; **12**: 416–424.
30. Speiser DE, Migliaccio M, Pittet MJ, *et al.* Human CD8⁺ T cells expressing HLA-DR and CD28 show telomerase activity and are distinct from cytolytic effector T cells. *Eur J Immunol* 2001; **31**: 459–466.
31. Arruvito L, Payaslian F, Baz P, *et al.* Identification and clinical relevance of naturally occurring human CD8⁺HLA-DR⁺ regulatory T cells. *J Immunol* 2014; **193**: 4469–4476.
32. Pfoertner S, Jeron A, Probst-Kepper M, *et al.* Signatures of human regulatory T cells: an encounter with old friends and new players. *Genome Biol* 2006; **7**: R54.
33. Kouo T, Huang L, Pucsek AB, *et al.* Galectin-3 shapes antitumor immune responses by suppressing CD8⁺ T cells via LAG-3 and inhibiting expansion of plasmacytoid dendritic cells. *Cancer Immunol Res* 2015; **3**: 412–423.
34. Abe R, Peng T, Sailors J, *et al.* Regulation of the CTL response by macrophage migration inhibitory factor. *J Immunol* 2001; **166**: 747–753.
35. Yan X, Orentas RJ, Johnson BD. Tumor-derived macrophage migration inhibitory factor (MIF) inhibits T lymphocyte activation. *Cytokine* 2006; **33**: 188–198.
36. Figueiredo CR, Azevedo RA, Mousdell S, *et al.* Blockade of MIF-CD74 signalling on macrophages and dendritic cells restores the antitumour immune response against metastatic melanoma. *Front Immunol* 2018; **9**: 1132.
37. Chen L, Diao L, Yang Y, *et al.* CD38-mediated immunosuppression as a mechanism of tumor cell escape from PD-1/PD-L1 blockade. *Cancer Discov* 2018; **8**: 1156–1175.
38. Bahri R, Bollinger A, Bollinger T, *et al.* Ectonucleotidase CD38 demarcates regulatory, memory-like CD8⁺ T cells with IFN- γ -mediated suppressor activities. *PLoS One* 2012; **7**: e45234.
39. Sledzinska A, Menger L, Bergerhoff K, *et al.* Negative immune checkpoints on T lymphocytes and their relevance to cancer immunotherapy. *Mol Oncol* 2015; **9**: 1936–1965.
40. Tang D, Lotze MT. Tumor immunity times out: TIM-3 and HMGB1. *Nat Immunol* 2012; **13**: 808–810.
41. Marin-Acevedo JA, Dholaria B, Soyano AE, *et al.* Next generation of immune checkpoint therapy in cancer: new developments and challenges. *J Hematol Oncol* 2018; **11**: 39.
42. Goldberg MV, Drake CG. LAG-3 in cancer immunotherapy. *Curr Top Microbiol Immunol* 2011; **344**: 269–278.
43. Allard B, Longhi MS, Robson SC, *et al.* The ectonucleotidases CD39 and CD73: novel checkpoint inhibitor targets. *Immunol Rev* 2017; **276**: 121–144.
44. Beavis PA, Stagg J, Darcy PK, *et al.* CD73: a potent suppressor of antitumor immune responses. *Trends Immunol* 2012; **33**: 231–237.
45. Martinez FO, Gordon S, Locati M, *et al.* Transcriptional profiling of the human monocyte-to-macrophage differentiation and polarization: new molecules and patterns of gene expression. *J Immunol* 2006; **177**: 7303–7311.
46. Ghoochani A, Schwarz MA, Yakubov E, *et al.* MIF-CD74 signaling impedes microglial M1 polarization and facilitates brain tumorigenesis. *Oncogene* 2016; **35**: 6246–6261.
47. Mills CD. M1 and M2 macrophages: oracles of health and disease. *Crit Rev Immunol* 2012; **32**: 463–488.
48. Simonetta F, Chiali A, Cordier C, *et al.* Increased CD127 expression on activated FOXP3⁺CD4⁺ regulatory T cells. *Eur J Immunol* 2010; **40**: 2528–2538.
49. Dunham RM, Cervasi B, Brenchley JM, *et al.* CD127 and CD25 expression defines CD4⁺ T cell subsets that are differentially depleted during HIV infection. *J Immunol* 2008; **180**: 5582–5592.
50. Yu N, Li X, Song W, *et al.* CD4⁺CD25⁺CD127^{low/-} T cells: a more specific Treg population in human peripheral blood. *Inflammation* 2012; **35**: 1773–1780.
51. Sharma S, Khosla R, David P, *et al.* CD4⁺CD25⁺CD127^{low} regulatory T cells play predominant anti-tumor suppressive role in hepatitis B virus-associated hepatocellular carcinoma. *Front Immunol* 2015; **6**: 49.
52. Lim KP, Chun NA, Ismail SM, *et al.* CD4⁺CD25^{hi}CD127^{low} regulatory T cells are increased in oral squamous cell carcinoma patients. *PLoS One* 2014; **9**: e103975.
53. Feng X, Zhang L, Acharya C, *et al.* Targeting CD38 suppresses induction and function of T regulatory cells to mitigate immunosuppression in multiple myeloma. *Clin Cancer Res* 2017; **23**: 4290–4300.
54. Sade-Feldman M, Jiao YJ, Chen JH, *et al.* Resistance to checkpoint blockade therapy through inactivation of antigen presentation. *Nat Commun* 2017; **8**: 1136.
55. Ferguson SD, Srinivasan VM, Heimberger AB. The role of STAT3 in tumor-mediated immune suppression. *J Neurooncol* 2015; **123**: 385–394.
56. Luo X, Li H, Ma L, *et al.* Expression of STING is increased in liver tissues from patients with NAFLD and promotes macrophage-mediated hepatic inflammation and fibrosis in mice. *Gastroenterology* 2018; **155**: 1971–1984.e1974.
57. Pai SG, Carneiro BA, Mota JM, *et al.* Wnt/beta-catenin pathway: modulating anticancer immune response. *J Hematol Oncol* 2017; **10**: 101.
58. Fu C, Liang X, Cui W, *et al.* β -Catenin in dendritic cells exerts opposite functions in cross-priming and maintenance of CD8⁺ T cells through regulation of IL-10. *Proc Natl Acad Sci U S A* 2015; **112**: 2823–2828.
59. Spranger S, Gajewski TF. A new paradigm for tumor immune escape: β -catenin-driven immune exclusion. *J Immunother Cancer* 2015; **3**: 43.
60. Lee YH, Martin-Orozco N, Zheng P, *et al.* Inhibition of the B7-H3 immune checkpoint limits tumor growth by enhancing cytotoxic lymphocyte function. *Cell Res* 2017; **27**: 1034–1045.
61. Holmgaard RB, Zamarin D, Munn DH, *et al.* Indoleamine 2,3-dioxygenase is a critical resistance mechanism in antitumor T cell immunotherapy targeting CTLA-4. *J Exp Med* 2013; **210**: 1389–1402.
62. Jenkins RW, Barbie DA, Flaherty KT. Mechanisms of resistance to immune checkpoint inhibitors. *Br J Cancer* 2018; **118**: 9–16.
63. Stålhammar G, Seregard S, Grossniklaus HE. Expression of immune checkpoint receptors indoleamine 2,3-dioxygenase and T cell Ig and ITIM domain in metastatic versus nonmetastatic choroidal melanoma. *Cancer Med* 2019; **8**: 2784–2792.
64. Farquhar N, Thornton S, Coupland SE, *et al.* Patterns of BAP1 protein expression provide insights into prognostic significance and the biology of uveal melanoma. *J Pathol Clin Res* 2018; **4**: 26–38.
65. Carbone M, Yang H, Pass HI, *et al.* BAP1 and cancer. *Nat Rev Cancer* 2013; **13**: 153–159.

66. Repp AC, Mayhew ES, Apte S, et al. Human uveal melanoma cells produce macrophage migration-inhibitory factor to prevent lysis by NK cells. *J Immunol* 2000; **165**: 710–715.
67. Leng L, Metz CN, Fang Y, et al. MIF signal transduction initiated by binding to CD74. *J Exp Med* 2003; **197**: 1467–1476.
68. Yaddanapudi K, Putty K, Rendon BE, et al. Control of tumor-associated macrophage alternative activation by macrophage migration inhibitory factor. *J Immunol* 2013; **190**: 2984–2993.
69. Costa-Silva B, Aiello NM, Ocean AJ, et al. Pancreatic cancer exosomes initiate pre-metastatic niche formation in the liver. *Nat Cell Biol* 2015; **17**: 816–826.
70. Yaddanapudi K, Rendon BE, Lamont G, et al. MIF is necessary for late-stage melanoma patient MDSC immune suppression and differentiation. *Cancer Immunol Res* 2016; **4**: 101–112.
71. Apte RS, Sinha D, Mayhew E, et al. Cutting edge: role of macrophage migration inhibitory factor in inhibiting NK cell activity and preserving immune privilege. *J Immunol* 1998; **160**: 5693–5696.
72. Schröder B. The multifaceted roles of the invariant chain CD74 – more than just a chaperone. *Biochim Biophys Acta* 2016; **1863**: 1269–1281.
73. Su H, Na N, Zhang X, et al. The biological function and significance of CD74 in immune diseases. *Inflamm Res* 2017; **66**: 209–216.
74. Berkova Z, Tao RH, Samaniego F. Milatuzumab – a promising new immunotherapeutic agent. *Expert Opin Investig Drugs* 2010; **19**: 141–149.
75. Govindan SV, Cardillo TM, Sharkey RM, et al. Milatuzumab–SN-38 conjugates for the treatment of CD74⁺ cancers. *Mol Cancer Ther* 2013; **12**: 968–978.
76. Ladanyi M, Sanchez Vega F, Zauderer M. Loss of BAP1 as a candidate predictive biomarker for immunotherapy of mesothelioma. *Genome Med* 2019; **11**:18.
77. Shrestha R, Nabavi N, Lin YY, et al. BAP1 haploinsufficiency predicts a distinct immunogenic class of malignant peritoneal mesothelioma. *Genome Med* 2019; **11**:8.
78. Arenzana TL, Lianoglou S, Seki A, et al. Tumor suppressor BAP1 is essential for thymic development and proliferative responses of T lymphocytes. *Sci Immunol* 2018; **3**:pii: eaal1953.
79. Mojic M, Takeda K, Hayakawa Y. The dark side of IFN- γ : its role in promoting cancer immunoevasion. *Int J Mol Sci* 2017; **19**: pii: E89.
80. Sansom DM. CD28, CTLA-4 and their ligands: who does what and to whom? *Immunology* 2000; **101**: 169–177.
81. Alegre ML, Noel PJ, Eisfelder BJ, et al. Regulation of surface and intracellular expression of CTLA4 on mouse T cells. *J Immunol* 1996; **157**: 4762–4770.
82. Freeman GJ, Lombard DB, Gimmi CD, et al. CTLA-4 and CD28 mRNA are coexpressed in most T cells after activation. Expression of CTLA-4 and CD28 mRNA does not correlate with the pattern of lymphokine production. *J Immunol* 1992; **149**: 3795–3801.
83. Linsley PS, Ledbetter JA. The role of the CD28 receptor during T cell responses to antigen. *Annu Rev Immunol* 1993; **11**: 191–212.
84. Amu S, Tarkowski A, Dörner T, et al. The human immunomodulatory CD25⁺ B cell population belongs to the memory B cell pool. *Scand J Immunol* 2007; **66**: 77–86.
85. Lino AC, Dang VD, Lampropoulou V, et al. LAG-3 inhibitory receptor expression identifies immunosuppressive natural regulatory plasma cells. *Immunity* 2018; **49**: 120–133.e129.
86. Pinyol R, Sia D, Llovet JM. Immune exclusion-Wnt/CTNBB1 class predicts resistance to immunotherapies in HCC. *Clin Cancer Res* 2019; **25**: 2021–2023.
87. Spranger S, Bao R, Gajewski TF. Melanoma-intrinsic β -catenin signalling prevents anti-tumour immunity. *Nature* 2015; **523**: 231–235.
- *88. Jeselsohn RM, Werner L, Regan MM, et al. Digital quantification of gene expression in sequential breast cancer biopsies reveals activation of an immune response. *PLoS One* 2013; **8**:e64225.
- *89. Kato Y, Tanaka Y, Hayashi M, et al. Involvement of CD166 in the activation of human gamma delta T cells by tumor cells sensitized with nonpeptide antigens. *J Immunol* 2006; **177**: 877–884.
- *90. Hassan NJ, Barclay AN, Brown MH. Frontline: optimal T cell activation requires the engagement of CD6 and CD166. *Eur J Immunol* 2004; **34**: 930–940.
- *91. Zhao Y, Niu C, Cui J. Gamma-delta ($\gamma\delta$) T cells: friend or foe in cancer development? *J Transl Med* 2018; **16**: 3.
- *92. Moog-Lutz C, Cave-Riant F, Guibal FC, et al. JAML, a novel protein with characteristics of a junctional adhesion molecule, is induced during differentiation of myeloid leukemia cells. *Blood* 2003; **102**: 3371–3378.
- *93. Scannell M, Flanagan MB, deStefani A, et al. Annexin-1 and peptide derivatives are released by apoptotic cells and stimulate phagocytosis of apoptotic neutrophils by macrophages. *J Immunol* 2007; **178**: 4595–4605.
- *94. Moraes LA, Ampomah PB, Lim LHK. Annexin A1 in inflammation and breast cancer: a new axis in the tumor microenvironment. *Cell Adh Migr* 2018; **12**: 417–423.
- *95. Ma Y, Galluzzi L, Zitvogel L, et al. Autophagy and cellular immune responses. *Immunity* 2013; **39**: 211–227.
96. Jinushi M, Chiba S, Baghdadi M, et al. ATM-mediated DNA damage signals mediate immune escape through integrin- $\alpha\beta$ 3-dependent mechanisms. *Cancer Res* 2012; **72**: 56–65.
- *97. Quigley M, Pereyra F, Nilsson B, et al. Transcriptional analysis of HIV-specific CD8⁺ T cells shows that PD-1 inhibits T cell function by upregulating BATF. *Nat Med* 2010; **16**: 1147–1151.
- *98. Adams JM, Cory S. The BCL-2 arbiters of apoptosis and their growing role as cancer targets. *Cell Death Differ* 2018; **25**: 27–36.
- *99. Kobayashi T, Hamaguchi Y, Hasegawa M, et al. B cells promote tumor immunity against B16F10 melanoma. *Am J Pathol* 2014; **184**: 3120–3129.
- *100. Bulla R, Tripodo C, Rami D, et al. C1q acts in the tumour microenvironment as a cancer-promoting factor independently of complement activation. *Nat Commun* 2016; **7**:10346.
- *101. Franchi L, Eigenbrod T, Munoz-Planillo R, et al. The inflammasome: a caspase-1-activation platform that regulates immune responses and disease pathogenesis. *Nat Immunol* 2009; **10**: 241–247.
- *102. Lee DJ, Du F, Chen SW, et al. Regulation and function of the caspase-1 in an inflammatory microenvironment. *J Invest Dermatol* 2015; **135**: 2012–2020.
- *103. Chen X, Liang H, Zhang J, et al. microRNAs are ligands of Toll-like receptors. *RNA* 2013; **19**: 737–739.
- *104. Takahashi K, Kawai T, Kumar H, et al. Roles of caspase-8 and caspase-10 in innate immune responses to double-stranded RNA. *J Immunol* 2006; **176**: 4520–4524.
- *105. Goping IS, Barry M, Liston P, et al. Granzyme B-induced apoptosis requires both direct caspase activation and relief of caspase inhibition. *Immunity* 2003; **18**: 355–365.
- *106. Su H, Bidere N, Zheng L, et al. Requirement for caspase-8 in NF- κ B activation by antigen receptor. *Science* 2005; **307**: 1465–1468.
- *107. Li J, Yuan W, Jiang S, et al. Prolyl-4-hydroxylase domain protein 2 controls NF- κ B/p65 transactivation and enhances the catabolic effects of inflammatory cytokines on cells of the nucleus pulposus. *J Biol Chem* 2015; **290**: 7195–7207.
- *108. Maruyama T, Kono K, Izawa S, et al. CCL17 and CCL22 chemokines within tumor microenvironment are related to infiltration of regulatory T cells in esophageal squamous cell carcinoma. *Dis Esophagus* 2010; **23**: 422–429.

- *109. Nagarsheth N, Wicha MS, Zou W. Chemokines in the cancer microenvironment and their relevance in cancer immunotherapy. *Nat Rev Immunol* 2017; **17**: 559–572.
- *110. Biswas SK, Mantovani A. Macrophage plasticity and interaction with lymphocyte subsets: cancer as a paradigm. *Nat Immunol* 2010; **11**: 889–896.
- *111. Patterson SJ, Pesenacker AM, Wang AY, *et al.* T regulatory cell chemokine production mediates pathogenic T cell attraction and suppression. *J Clin Invest* 2016; **126**: 1039–1051.
- *112. Gonzalez-Martin A, Gomez L, Lustgarten J, *et al.* Maximal T cell-mediated antitumor responses rely upon CCR5 expression in both CD4⁺ and CD8⁺ T cells. *Cancer Res* 2011; **71**: 5455–5466.
- *113. Marques RE, Guabiraba R, Russo RC, *et al.* Targeting CCL5 in inflammation. *Expert Opin Ther Targets* 2013; **17**: 1439–1460.
- *114. Qian BZ, Li J, Zhang H, *et al.* CCL2 recruits inflammatory monocytes to facilitate breast-tumour metastasis. *Nature* 2011; **475**: 222–225.
- *115. Curiel TJ, Coukos G, Zou L, *et al.* Specific recruitment of regulatory T cells in ovarian carcinoma fosters immune privilege and predicts reduced survival. *Nat Med* 2004; **10**: 942–949.
- *116. Berraondo P, Sanmamed MF, Ochoa MC, *et al.* Cytokines in clinical cancer immunotherapy. *Br J Cancer* 2019; **120**: 6–15.
- *117. Otero K, Vecchi A, Hirsch E, *et al.* Nonredundant role of CCRL2 in lung dendritic cell trafficking. *Blood* 2010; **116**: 2942–2949.
- *118. Bachmann MF, Barner M, Kopf M. CD2 sets quantitative thresholds in T cell activation. *J Exp Med* 1999; **190**: 1383–1392.
- *119. Zhou T, Chen Y, Hao L, *et al.* DC-SIGN and immunoregulation. *Cell Mol Immunol* 2006; **3**: 279–283.
- *120. Samelson LE, Patel MD, Weissman AM, *et al.* Antigen activation of murine T cells induces tyrosine phosphorylation of a polypeptide associated with the T cell antigen receptor. *Cell* 1986; **46**: 1083–1090.
- *121. Baniyash M, Garcia-Morales P, Luong E, *et al.* The T cell antigen receptor zeta chain is tyrosine phosphorylated upon activation. *J Biol Chem* 1988; **263**: 18225–18230.
- *122. D’Oro U, Munitic I, Chacko G, *et al.* Regulation of constitutive TCR internalization by the zeta-chain. *J Immunol* 2002; **169**: 6269–6278.
- *123. Irving BA, Weiss A. The cytoplasmic domain of the T cell receptor zeta chain is sufficient to couple to receptor-associated signal transduction pathways. *Cell* 1991; **64**: 891–901.
- *124. Hendriks J, Gravestien LA, Tesselaar K, *et al.* CD27 is required for generation and long-term maintenance of T cell immunity. *Nat Immunol* 2000; **1**: 433–440.
- *125. O’Neill RE, Du W, Mohamadpour H, *et al.* T cell-derived CD70 delivers an immune checkpoint function in inflammatory T cell responses. *J Immunol* 2017; **199**: 3700–3710.
- *126. Klebanoff CA, Gattinoni L, Restifo NP. CD8⁺ T-cell memory in tumor immunology and immunotherapy. *Immunol Rev* 2006; **211**: 214–224.
- *127. Sandoval-Montes C, Santos-Argumedo L. CD38 is expressed selectively during the activation of a subset of mature T cells with reduced proliferation but improved potential to produce cytokines. *J Leukoc Biol* 2005; **77**: 513–521.
- *128. Patton DT, Wilson MD, Rowan WC, *et al.* The PI3K p110 δ regulates expression of CD38 on regulatory T cells. *PLoS One* 2011; **6**: e17359.
- *129. Bahri R, Bollinger A, Bollinger T, *et al.* Ectonucleotidase CD38 demarcates regulatory, memory-like CD8⁺ T cells with IFN- γ -mediated suppressor activities. *PLoS One* 2012; **7**: e45234.
- *130. Pahima H, Puzzovio PG, Levi-Schaffer F. 2B4 and CD48: a powerful couple of the immune system. *Clin Immunol* 2019; **204**: 64–68.
- *131. Tabbekh M, Mokrani-Hammani M, Bismuth G, *et al.* T-cell modulatory properties of CD5 and its role in antitumor immune responses. *Oncimmunology* 2013; **2**: e22841.
- *132. Todros-Dawda I, Kveberg L, Vaage JT, *et al.* The tetraspanin CD53 modulates responses from activating NK cell receptors, promoting LFA-1 activation and dampening NK cell effector functions. *PLoS One* 2014; **9**: e97844.
- *133. Aandahl EM, Sandberg JK, Beckerman KP, *et al.* CD7 is a differentiation marker that identifies multiple CD8 T cell effector subsets. *J Immunol* 2003; **170**: 2349–2355.
- *134. Shevach EM. Mechanisms of Foxp3⁺ T regulatory cell-mediated suppression. *Immunity* 2009; **30**: 636–645.
- *135. Yan Q, Malashkevich VN, Fedorov A, *et al.* Structure of CD84 provides insight into SLAM family function. *Proc Natl Acad Sci U S A* 2007; **104**: 10583–10588.
- *136. Munn DH, Sharma MD, Mellor AL. Ligation of B7-1/B7-2 by human CD4⁺ T cells triggers indoleamine 2,3-dioxygenase activity in dendritic cells. *J Immunol* 2004; **172**: 4100–4110.
- *137. Paust S, Lu L, McCarty N, *et al.* Engagement of B7 on effector T cells by regulatory T cells prevents autoimmune disease. *Proc Natl Acad Sci U S A* 2004; **101**: 10398–10403.
- *138. Mellman I, Steinman RM. Dendritic cells: specialized and regulated antigen processing machines. *Cell* 2001; **106**: 255–258.
- *139. Zhang N, Bevan MJ. CD8⁺ T cells: foot soldiers of the immune system. *Immunity* 2011; **35**: 161–168.
- *140. Arcaro A, Gregoire C, Bakker TR, *et al.* CD8 β endows CD8 with efficient coreceptor function by coupling T cell receptor/CD3 to raft-associated CD8/p56^{lck} complexes. *J Exp Med* 2001; **194**: 1485–1495.
- *141. Reyes R, Cardenas B, Machado-Pineda Y, *et al.* Tetraspanin CD9: a key regulator of cell adhesion in the immune system. *Front Immunol* 2018; **9**: 863.
- *142. Dougall WC, Kurtulus S, Smyth MJ, *et al.* TIGIT and CD96: new checkpoint receptor targets for cancer immunotherapy. *Immunol Rev* 2017; **276**: 112–120.
- *143. Meyer-Wentrup F, Benitez-Ribas D, Tacke PJ, *et al.* Targeting DCIR on human plasmacytoid dendritic cells results in antigen presentation and inhibits IFN- α production. *Blood* 2008; **111**: 4245–4253.
- *144. Long X, Li Y, Qiu S, *et al.* MiR-582-5p/miR-590-5p targeted CREB1/CREB5-NF- κ B signaling and caused opioid-induced immunosuppression in human monocytes. *Transl Psychiatry* 2016; **6**: e757.
- *145. Rooney MS, Shukla SA, Wu CJ, *et al.* Molecular and genetic properties of tumors associated with local immune cytolytic activity. *Cell* 2015; **160**: 48–61.
- *146. Ondr JK, Pham CT. Characterization of murine cathepsin W and its role in cell-mediated cytotoxicity. *J Biol Chem* 2004; **279**: 27525–27533.
- *147. Liu M, Guo S, Stiles JK. The emerging role of CXCL10 in cancer (Review). *Oncol Lett* 2011; **2**: 583–589.
- *148. Sokol CL, Luster AD. The chemokine system in innate immunity. *Cold Spring Harb Perspect Biol* 2015; **7**: pii: a016303.
- *149. David JM, Dominguez C, Hamilton DH, *et al.* The IL-8/IL-8R axis: a double agent in tumor immune resistance. *Vaccines* 2016; **4**: pii: E22.
- *150. Szebeni GJ, Vizler C, Kitajka K, *et al.* Inflammation and cancer: extra- and intracellular determinants of tumor-associated macrophages as tumor promoters. *Mediators Inflamm* 2017; **2017**: 9294018.
- *151. Rolny C, Capparuccia L, Casazza A, *et al.* The tumor suppressor semaphorin 3B triggers a prometastatic program mediated by interleukin 8 and the tumor microenvironment. *J Exp Med* 2008; **205**: 1155–1171.
- *152. Jehs T, Faber C, Juel HB, *et al.* Inflammation-induced chemokine expression in uveal melanoma cell lines stimulates monocyte chemotaxis. *Invest Ophthalmol Vis Sci* 2014; **55**: 5169–5175.
- *153. Groom JR, Luster AD. CXCR3 in T cell function. *Exp Cell Res* 2011; **317**: 620–631.

- *154. Gao Q, Zhao YJ, Wang XY, *et al.* CXCR6 upregulation contributes to a proinflammatory tumor microenvironment that drives metastasis and poor patient outcomes in hepatocellular carcinoma. *Cancer Res* 2012; **72**: 3546–3556.
- *155. Darash-Yahana M, Gillespie JW, Hewitt SM, *et al.* The chemokine CXCL16 and its receptor, CXCR6, as markers and promoters of inflammation-associated cancers. *PLoS One* 2009; **4**: e6695.
- *156. Nathan C, Cunningham-Bussell A. Beyond oxidative stress: an immunologist's guide to reactive oxygen species. *Nat Rev Immunol* 2013; **13**: 349–361.
- *157. Bustamante J, Arias AA, Vogt G, *et al.* Germline *CYBB* mutations that selectively affect macrophages in kindreds with X-linked predisposition to tuberculous mycobacterial disease. *Nat Immunol* 2011; **12**: 213–221.
- *158. Ohnuma K, Hatano R, Morimoto C. DPP4 in anti-tumor immunity: going beyond the enzyme. *Nat Immunol* 2015; **16**: 791–792.
- *159. Williams JB, Horton BL, Zheng Y, *et al.* The EGR2 targets LAG-3 and 4-1BB describe and regulate dysfunctional antigen-specific CD8⁺ T cells in the tumor microenvironment. *J Exp Med* 2017; **214**: 381–400.
- *160. Gao Y, Souza-Fonseca-Guimaraes F, Bald T, *et al.* Tumor immunoevasion by the conversion of effector NK cells into type 1 innate lymphoid cells. *Nat Immunol* 2017; **18**: 1004–1015.
- *161. Mancardi DA, Albanesi M, Jonsson F, *et al.* The high-affinity human IgG receptor FcγRI (CD64) promotes IgG-mediated inflammation, anaphylaxis, and antitumor immunotherapy. *Blood* 2013; **121**: 1563–1573.
- *162. Bournazos S, Wang TT, Ravetch JV. The role and function of Fcγ receptors on myeloid cells. *Microbiol Spectr* 2016; **4**. <https://doi.org/10.1128/microbiolspec.MCHD-0045-2016>.
- *163. Romee R, Foley B, Lenvik T, *et al.* NK cell CD16 surface expression and function is regulated by a disintegrin and metalloprotease-17 (ADAM17). *Blood* 2013; **121**: 3599–3608.
- *164. Bjorkstrom NK, Gonzalez VD, Malmberg KJ, *et al.* Elevated numbers of FcγRIIIA⁺ (CD16⁺) effector CD8 T cells with NK cell-like function in chronic hepatitis C virus infection. *J Immunol* 2008; **181**: 4219–4228.
- *165. Waskow C, Liu K, Darrasse-Jeze G, *et al.* The receptor tyrosine kinase Flt3 is required for dendritic cell development in peripheral lymphoid tissues. *Nat Immunol* 2008; **9**: 676–683.
- *166. Moraes LA, Kar S, Foo SL, *et al.* Annexin-A1 enhances breast cancer growth and migration by promoting alternative macrophage polarization in the tumour microenvironment. *Sci Rep* 2017; **7**: 17925.
- *167. Waechter V, Schmid M, Herova M, *et al.* Characterization of the promoter and the transcriptional regulation of the *lipoxin A4 receptor (FPR2/ALX)* gene in human monocytes and macrophages. *J Immunol* 2012; **188**: 1856–1867.
- *168. Wan YY. GATA3: a master of many trades in immune regulation. *Trends Immunol* 2014; **35**: 233–242.
- *169. Cao X, Cai SF, Fehniger TA, *et al.* Granzyme B and perforin are important for regulatory T cell-mediated suppression of tumor clearance. *Immunity* 2007; **27**: 635–646.
- *170. Arias M, Martinez-Lostao L, Santiago L, *et al.* The untold story of granzymes in oncoimmunology: novel opportunities with old acquaintances. *Trends Cancer* 2017; **3**: 407–422.
- *171. Martinez-Lostao L, Anel A, Pardo J. How do cytotoxic lymphocytes kill cancer cells? *Clin Cancer Res* 2015; **21**: 5047–5056.
- *172. Bovenschen N, Kummer JA. Orphan granzymes find a home. *Immunol Rev* 2010; **235**: 117–127.
- *173. Chowdhury D, Lieberman J. Death by a thousand cuts: granzyme pathways of programmed cell death. *Annu Rev Immunol* 2008; **26**: 389–420.
- *174. Plitas G, Konopacki C, Wu K, *et al.* Regulatory T cells exhibit distinct features in human breast cancer. *Immunity* 2016; **45**: 1122–1134.
- *175. Bailey SR, Nelson MH, Majchrzak K, *et al.* Human CD26^{high} T cells elicit tumor immunity against multiple malignancies via enhanced migration and persistence. *Nat Commun* 2017; **8**: 1961.
- *176. van Essen TH, van Pelt SI, Bronkhorst IH, *et al.* Upregulation of HLA expression in primary uveal melanoma by infiltrating leukocytes. *PLoS One* 2016; **11**: e0164292.
- *177. Doebele RC, Busch R, Scott HM, *et al.* Determination of the HLA-DM interaction site on HLA-DR molecules. *Immunity* 2000; **13**: 517–527.
- *178. Mellins ED, Stern LJ. HLA-DM and HLA-DO, key regulators of MHC-II processing and presentation. *Curr Opin Immunol* 2014; **26**: 115–122.
- *179. Chen X, Jensen PE. MHC class II antigen presentation and immunological abnormalities due to deficiency of MHC class II and its associated genes. *Exp Mol Pathol* 2008; **85**: 40–44.
- *180. Hake SB, Tobin HM, Steimle V, *et al.* Comparison of the transcriptional regulation of classical and non-classical MHC class II genes. *Eur J Immunol* 2003; **33**: 2361–2371.
- *181. Reith W, LeibundGut-Landmann S, Waldburger JM. Regulation of MHC class II gene expression by the class II transactivator. *Nat Rev Immunol* 2005; **5**: 793–806.
- *182. Pino-Otin MR, Juan M, de la Fuente MA, *et al.* CD50 (intercellular adhesion molecule-3) is expressed at higher levels on memory than on naive human T cells but induces a similar calcium mobilization on both subsets. *Tissue Antigens* 1995; **46**: 32–44.
- *183. Chien CH, Chiang BL. Regulatory T cells induced by B cells: a novel subpopulation of regulatory T cells. *J Biomed Sci* 2017; **24**: 86.
- *184. Chen PW, Mellon JK, Mayhew E, *et al.* Uveal melanoma expression of indoleamine 2,3-dioxygenase: establishment of an immune privileged environment by tryptophan depletion. *Exp Eye Res* 2007; **85**: 617–625.
- *185. Oliva M, Rullan AJ, Piulats JM. Uveal melanoma as a target for immune-therapy. *Ann Transl Med* 2016; **4**: 172.
- *186. Munn DH, Mellor AL. Indoleamine 2,3-dioxygenase and tumor-induced tolerance. *J Clin Invest* 2007; **117**: 1147–1154.
- *187. Mellor AL, Lemos H, Huang L. Indoleamine 2,3-dioxygenase and tolerance: where are we now? *Front Immunol* 2017; **8**: 1360.
- *188. Munn DH, Mellor AL. IDO and tolerance to tumors. *Trends Mol Med* 2004; **10**: 15–18.
- *189. Zoso A, Mazza EM, Biccato S, *et al.* Human fibrocytic myeloid-derived suppressor cells express IDO and promote tolerance via Treg-cell expansion. *Eur J Immunol* 2014; **44**: 3307–3319.
- *190. Hervas-Stubbs S, Perez-Gracia JL, Rouzaut A, *et al.* Direct effects of type I interferons on cells of the immune system. *Clin Cancer Res* 2011; **17**: 2619–2627.
- *191. Katlinski KV, Gui J, Katlinskaya YV, *et al.* Inactivation of interferon receptor promotes the establishment of immune privileged tumor microenvironment. *Cancer Cell* 2017; **31**: 194–207.
- *192. Taylor A, Verhagen J, Blaser K, *et al.* Mechanisms of immune suppression by interleukin-10 and transforming growth factor-beta: the role of T regulatory cells. *Immunology* 2006; **117**: 433–442.
- *193. Yan J, Smyth MJ, Teng MWL. Interleukin (IL)-12 and IL-23 and their conflicting roles in cancer. *Cold Spring Harb Perspect Biol* 2018; **10**: pii: a028530.
- *194. Marquis JF, Kapoustina O, Langlais D, *et al.* Interferon regulatory factor 8 regulates pathways for antigen presentation in myeloid cells and during tuberculosis. *PLoS Genet* 2011; **7**: e1002097.
- *195. Terabe M, Park JM, Berzofsky JA. Role of IL-13 in regulation of anti-tumor immunity and tumor growth. *Cancer Immunol Immunother* 2004; **53**: 79–85.
- *196. Steel JC, Waldmann TA, Morris JC. Interleukin-15 biology and its therapeutic implications in cancer. *Trends Pharmacol Sci* 2012; **33**: 35–41.

- *197. Terme M, Ullrich E, Aymeric L, *et al.* IL-18 induces PD-1-dependent immunosuppression in cancer. *Cancer Res* 2011; **71**: 5393–5399.
- *198. Santegoets SJ, Turksma AW, Powell DJ Jr, *et al.* IL-21 in cancer immunotherapy: at the right place at the right time. *Oncoimmunology* 2013; **2**: e24522.
- *199. Stolfi C, Pallone F, Macdonald TT, *et al.* Interleukin-21 in cancer immunotherapy: friend or foe? *Oncoimmunology* 2012; **1**: 351–354.
- *200. Ma YF, Ren Y, Wu CJ, *et al.* Interleukin (IL)-24 transforms the tumor microenvironment and induces anticancer immunity in a murine model of colon cancer. *Mol Immunol* 2016; **75**: 11–20.
- *201. Diveu C, McGeachy MJ, Boniface K, *et al.* IL-27 blocks RORc expression to inhibit lineage commitment of Th17 cells. *J Immunol* 2009; **182**: 5748–5756.
- *202. Fabbi M, Carbotti G, Ferrini S. Dual roles of IL-27 in cancer biology and immunotherapy. *Mediators Inflamm* 2017; **2017**: 3958069.
- *203. Malek TR, Castro I. Interleukin-2 receptor signaling: at the interface between tolerance and immunity. *Immunity* 2010; **33**: 153–165.
- *204. Ohmatsu H, Humme D, Gonzalez J, *et al.* IL-32 induces indoleamine 2,3-dioxygenase⁺CD1c⁺ dendritic cells and indoleamine 2,3-dioxygenase⁺CD163⁺ macrophages: relevance to mycosis fungoides progression. *Oncoimmunology* 2017; **6**: e1181237.
- *205. Tsukamoto H, Fujieda K, Senju S, *et al.* Immune-suppressive effects of interleukin-6 on T-cell-mediated anti-tumor immunity. *Cancer Sci* 2018; **109**: 523–530.
- *206. Mazzucchelli R, Hixon JA, Spolski R, *et al.* Development of regulatory T cells requires IL-7R α stimulation by IL-7 or TSLP. *Blood* 2008; **112**: 3283–3292.
- *207. Espert L, Rey C, Gonzalez L, *et al.* The exonuclease ISG20 is directly induced by synthetic dsRNA via NF- κ B and IRF1 activation. *Oncogene* 2004; **23**: 4636–4640.
- *208. Lee W, Kim HS, Baek SY, *et al.* Transcription factor IRF8 controls Th1-like regulatory T-cell function. *Cell Mol Immunol* 2016; **13**: 785–794.
- *209. Lau CM, Adams NM, Geary CD, *et al.* Epigenetic control of innate and adaptive immune memory. *Nat Immunol* 2018; **19**: 963–972.
- *210. Cheuk S, Schlums H, Gallais Serezal I, *et al.* CD49a expression defines tissue-resident CD8⁺ T cells poised for cytotoxic function in human skin. *Immunity* 2017; **46**: 287–300.
- *211. Wu X, Wu P, Shen Y, *et al.* CD8⁺ resident memory T cells and viral infection. *Front Immunol* 2018; **9**: 2093.
- *212. Zeltz C, Gullberg D. The integrin–collagen connection – a glue for tissue repair? *J Cell Sci* 2016; **129**: 1284.
- *213. Amsen D, van Gisbergen K, Hombrink P, *et al.* Tissue-resident memory T cells at the center of immunity to solid tumors. *Nat Immunol* 2018; **19**: 538–546.
- *214. Vicente R, Quentin J, Mausset-Bonnefont AL, *et al.* Nonclassical CD4⁺CD49b⁺ regulatory T cells as a better alternative to conventional CD4⁺CD25⁺ T cells to dampen arthritis severity. *J Immunol* 2016; **196**: 298–309.
- *215. Yang Q, Bavi P, Wang JY, *et al.* Immuno-proteomic discovery of tumor tissue autoantigens identifies olfactomedin 4, CD11b, and integrin alpha-2 as markers of colorectal cancer with liver metastases. *J Proteomics* 2017; **168**: 53–65.
- *216. Christiaansen AF, Dixit UG, Coler RN, *et al.* CD11a and CD49d enhance the detection of antigen-specific T cells following human vaccination. *Vaccine* 2017; **35**: 4255–4261.
- *217. Ammon C, Meyer SP, Schwarzfischer L, *et al.* Comparative analysis of integrin expression on monocyte-derived macrophages and monocyte-derived dendritic cells. *Immunology* 2000; **100**: 364–369.
- *218. Hoek K, Rimm DL, Williams KR, *et al.* Expression profiling reveals novel pathways in the transformation of melanocytes to melanomas. *Cancer Res* 2004; **64**: 5270–5282.
- *219. Yanguas A, Garasa S, Teijeira A, *et al.* ICAM-1–LFA-1 dependent CD8⁺ T-lymphocyte aggregation in tumor tissue prevents recirculation to draining lymph nodes. *Front Immunol* 2018; **9**: 2084.
- *220. Sharma A, Lawry SM, Klein BS, *et al.* LFA-1 ligation by high-density ICAM-1 is sufficient to activate IFN- γ release by innate T lymphocytes. *J Immunol* 2018; **201**: 2452–2461.
- *221. Raab M, Lu Y, Kohler K, *et al.* LFA-1 activates focal adhesion kinases FAK1/PYK2 to generate LAT–GRB2–SKAP1 complexes that terminate T-cell conjugate formation. *Nat Commun* 2017; **8**: 16001.
- *222. Saalbach A, Wetzel A, Hausteiner UF, *et al.* Interaction of human Thy-1 (CD90) with the integrin α v β 3 (CD51/CD61): an important mechanism mediating melanoma cell adhesion to activated endothelium. *Oncogene* 2005; **24**: 4710–4720.
- *223. Karachaliou N, Pilotto S, Bria E, *et al.* Platelets and their role in cancer evolution and immune system. *Transl Lung Cancer Res* 2015; **4**: 713–720.
- *224. Huang W, Jeong AR, Kannan AK, *et al.* IL-2-inducible T cell kinase tunes T regulatory cell development and is required for suppressive function. *J Immunol* 2014; **193**: 2267–2272.
- *225. Bakker AB, Phillips JH, Figdor CG, *et al.* Killer cell inhibitory receptors for MHC class I molecules regulate lysis of melanoma cells mediated by NK cells, gamma delta T cells, and antigen-specific CTL. *J Immunol* 1998; **160**: 5239–5245.
- *226. Baixeras E, Huard B, Miossec C, *et al.* Characterization of the lymphocyte activation gene 3-encoded protein. A new ligand for human leukocyte antigen class II antigens. *J Exp Med* 1992; **176**: 327–337.
- *227. Huard B, Prigent P, Tournier M, *et al.* CD4/major histocompatibility complex class II interaction analyzed with CD4- and lymphocyte activation gene-3 (LAG-3)-Ig fusion proteins. *Eur J Immunol* 1995; **25**: 2718–2721.
- *228. Davis SJ, van der Merwe PA. Lck and the nature of the T cell receptor trigger. *Trends Immunol* 2011; **32**: 1–5.
- *229. Wang C, Morley SC, Donermeyer D, *et al.* Actin-bundling protein L-plastin regulates T cell activation. *J Immunol* 2010; **185**: 7487–7497.
- *230. Morley SC, Wang C, Lo WL, *et al.* The actin-bundling protein L-plastin dissociates CCR7 proximal signaling from CCR7-induced motility. *J Immunol* 2010; **184**: 3628–3638.
- *231. Foran E, McWilliam P, Kelleher D, *et al.* The leukocyte protein L-plastin induces proliferation, invasion and loss of E-cadherin expression in colon cancer cells. *Int J Cancer* 2006; **118**: 2098–2104.
- *232. Chen HY, Fermin A, Vardhana S, *et al.* Galectin-3 negatively regulates TCR-mediated CD4⁺ T-cell activation at the immunological synapse. *Proc Natl Acad Sci U S A* 2009; **106**: 14496–14501.
- *233. Albregues J, Bourget I, Pons C, *et al.* LIF mediates proinvasive activation of stromal fibroblasts in cancer. *Cell Rep* 2014; **7**: 1664–1678.
- *234. Barkal AA, Weiskopf K, Kao KS, *et al.* Engagement of MHC class I by the inhibitory receptor LILRB1 suppresses macrophages and is a target of cancer immunotherapy. *Nat Immunol* 2018; **19**: 76–84.
- *235. Chen HM, van der Touw W, Wang YS, *et al.* Blocking immunoinhibitory receptor LILRB2 reprograms tumor-associated myeloid cells and promotes antitumor immunity. *J Clin Invest* 2018; **128**: 5647–5662.
- *236. Nirmal AJ, Regan T, Shih BB, *et al.* Immune cell gene signatures for profiling the microenvironment of solid tumors. *Cancer Immunol Res* 2018; **6**: 1388–1400.
- *237. Bjordahl RL, Steidl C, Gascoyne RD, *et al.* Lymphotoxin network pathways shape the tumor microenvironment. *Curr Opin Immunol* 2013; **25**: 222–229.
- *238. Wang H, Peters T, Sindrilaru A, *et al.* TGF- β -dependent suppressive function of Tregs requires wild-type levels of CD18 in a mouse model of psoriasis. *J Clin Invest* 2008; **118**: 2629–2639.

- *239. Veillette A. SLAM-family receptors: immune regulators with or without SAP-family adaptors. *Cold Spring Harb Perspect Biol* 2010; **2**:a002469.
- *240. Xu Y, Harder KW, Huntington ND, et al. Lyn tyrosine kinase: accentuating the positive and the negative. *Immunity* 2005; **22**: 9–18.
- *241. Horikawa K, Nishizumi H, Umemori H, et al. Distinctive roles of Fyn and Lyn in IgD- and IgM-mediated signaling. *Int Immunol* 1999; **11**: 1441–1449.
- *242. Yasue T, Nishizumi H, Aizawa S, et al. A critical role of Lyn and Fyn for B cell responses to CD38 ligation and interleukin 5. *Proc Natl Acad Sci U S A* 1997; **94**: 10307–10312.
- *243. Mehlhop-Williams ER, Bevan MJ. Memory CD8⁺ T cells exhibit increased antigen threshold requirements for recall proliferation. *J Exp Med* 2014; **211**: 345–356.
- *244. Skrzypczynska KM, Zhu JW, Weiss A. Positive regulation of Lyn kinase by CD148 is required for B cell receptor signaling in B1 but not B2 B cells. *Immunity* 2016; **45**: 1232–1244.
- *245. Caunt CJ, Sale MJ, Smith PD, et al. MEK1 and MEK2 inhibitors and cancer therapy: the long and winding road. *Nat Rev Cancer* 2015; **15**: 577–592.
- *246. Karki R, Man SM, Kanneganti TD. Inflammasomes and cancer. *Cancer Immunol Res* 2017; **5**: 94–99.
- *247. Centola M, Wood G, Frucht DM, et al. The gene for familial Mediterranean fever, *MEFV*, is expressed in early leukocyte development and is regulated in response to inflammatory mediators. *Blood* 2000; **95**: 3223–3231.
- *248. Broz P, Dixit VM. Inflammasomes: mechanism of assembly, regulation and signalling. *Nat Rev Immunol* 2016; **16**: 407–420.
- *249. Lepore M, Mori L, De Libero G. The conventional nature of non-MHC-restricted T cells. *Front Immunol* 2018; **9**: 1365.
- *250. Huang W, He W, Shi X, et al. The role of CD1d and MR1 restricted T cells in the liver. *Front Immunol* 2018; **9**: 2424.
- *251. van de Veerdonk FL, Dinarello CA. Deficient autophagy unravels the ROS paradox in chronic granulomatous disease. *Autophagy* 2014; **10**: 1141–1142.
- *252. Graham DB, Becker CE, Doan A, et al. Functional genomics identifies negative regulatory nodes controlling phagocyte oxidative burst. *Nat Commun* 2015; **6**:7838.
- *253. Li XQ, Li L, Xiao CH, et al. *NEFL* mRNA expression level is a prognostic factor for early-stage breast cancer patients. *PLoS One* 2012; **7**:e31146.
- *254. Huang Z, Zhuo Y, Shen Z, et al. The role of *NEFL* in cell growth and invasion in head and neck squamous cell carcinoma cell lines. *J Oral Pathol Med* 2014; **43**: 191–198.
- *255. van Beek JG, Koopmans AE, Vaarwater J, et al. The prognostic value of extraocular extension in relation to monosomy 3 and gain of chromosome 8q in uveal melanoma. *Invest Ophthalmol Vis Sci* 2014; **55**: 1284–1291.
- *256. Shou J, Jing J, Xie J, et al. Nuclear factor of activated T cells in cancer development and treatment. *Cancer Lett* 2015; **361**: 174–184.
- *257. Oukka M, Ho IC, de la Brousse FC, et al. The transcription factor NFAT4 is involved in the generation and survival of T cells. *Immunity* 1998; **9**: 295–304.
- *258. Ranger AM, Oukka M, Rengarajan J, et al. Inhibitory function of two NFAT family members in lymphoid homeostasis and Th2 development. *Immunity* 1998; **9**: 627–635.
- *259. Yoshihama S, Vijayan S, Sidiq T, et al. *NLR5/CITA*: a key player in cancer immune surveillance. *Trends Cancer* 2017; **3**: 28–38.
- *260. Pauleau AL, Murray PJ. Role of Nod2 in the response of macrophages to Toll-like receptor agonists. *Mol Cell Biol* 2003; **23**: 7531–7539.
- *261. Lessard AJ, LeBel M, Egarnes B, et al. Triggering of NOD2 receptor converts inflammatory Ly6C^{high} into Ly6C^{low} monocytes with patrolling properties. *Cell Rep* 2017; **20**: 1830–1843.
- *262. Chaudhary B, Khaled YS, Ammori BJ, et al. Neuropilin 1: function and therapeutic potential in cancer. *Cancer Immunol Immunother* 2014; **63**: 81–99.
- *263. Kohler A, Hurt E. Gene regulation by nucleoporins and links to cancer. *Mol Cell* 2010; **38**: 6–15.
- *264. Wei SC, Duffy CR, Allison JP. Fundamental mechanisms of immune checkpoint blockade therapy. *Cancer Discov* 2018; **8**: 1069–1086.
- *265. Marelli-Berg FM, Clement M, Mauro C, et al. An immunologist's guide to CD31 function in T-cells. *J Cell Sci* 2013; **126**: 2343–2352.
- *266. Ma L, Cheung KC, Kishore M, et al. CD31 exhibits multiple roles in regulating T lymphocyte trafficking *in vivo*. *J Immunol* 2012; **189**: 4104–4111.
- *267. Manrique SZ, Correa MA, Hoelzinger DB, et al. Foxp3-positive macrophages display immunosuppressive properties and promote tumor growth. *J Exp Med* 2011; **208**: 1485–1499.
- *268. Corcoran L, Emslie D, Kratina T, et al. Oct2 and Obf1 as facilitators of B:T cell collaboration during a humoral immune response. *Front Immunol* 2014; **5**: 108.
- *269. Gondek DC, Lu LF, Quezada SA, et al. Cutting edge: contact-mediated suppression by CD4⁺CD25⁺ regulatory cells involves a granzyme B-dependent, perforin-independent mechanism. *J Immunol* 2005; **174**: 1783–1786.
- *270. Wen T, Rothenberg ME. The regulatory function of eosinophils. *Microbiol Spectr* 2016; **4**. <https://doi.org/10.1128/microbiolspec.MCHD-0020-2015>.
- *271. Odemuyiwa SO, Ghahary A, Li Y, et al. Cutting edge: human eosinophils regulate T cell subset selection through indoleamine 2,3-dioxygenase. *J Immunol* 2004; **173**: 5909–5913.
- *272. Rouette A, Trofimov A, Haberl D, et al. Expression of immunoproteasome genes is regulated by cell-intrinsic and -extrinsic factors in human cancers. *Sci Rep* 2016; **6**:34019.
- *273. Basler M, Kirk CJ, Groettrup M. The immunoproteasome in antigen processing and other immunological functions. *Curr Opin Immunol* 2013; **25**: 74–80.
- *274. Kalinski P. Regulation of immune responses by prostaglandin E2. *J Immunol* 2012; **188**: 21–28.
- *275. Thomas ML. The leukocyte common antigen family. *Annu Rev Immunol* 1989; **7**: 339–369.
- *276. Voon DC, Hor YT, Ito Y. The RUNX complex: reaching beyond haematopoiesis into immunity. *Immunology* 2015; **146**: 523–536.
- *277. Taniuchi I, Osato M, Egawa T, et al. Differential requirements for Runx proteins in CD4 repression and epigenetic silencing during T lymphocyte development. *Cell* 2002; **111**: 621–633.
- *278. Lorsbach RB, Moore S, Ang SO, et al. Role of RUNX1 in adult hematopoiesis: analysis of RUNX1-IRES-GFP knock-in mice reveals differential lineage expression. *Blood* 2004; **103**: 2522–2529.
- *279. Calpe S, Wang N, Romero X, et al. The SLAM and SAP gene families control innate and adaptive immune responses. *Adv Immunol* 2008; **97**: 177–250.
- *280. Veillette A. NK cell regulation by SLAM family receptors and SAP-related adapters. *Immunol Rev* 2006; **214**: 22–34.
- *281. Pedraza-Alva G, Merida LB, del Rio R, et al. CD43 regulates the threshold for T cell activation by targeting Cbl functions. *IUBMB Life* 2011; **63**: 940–948.
- *282. Park JK, Rosenstein YJ, Remold-O'Donnell E, et al. Enhancement of T-cell activation by the CD43 molecule whose expression is defective in Wiskott–Aldrich syndrome. *Nature* 1991; **350**: 706–709.
- *283. Hasegawa K, Tanaka S, Fujiki F, et al. Glycosylation status of CD43 protein is associated with resistance of leukemia cells to CTL-mediated cytolysis. *PLoS One* 2016; **11**: e0152326.

- *284. He YW, Bevan MJ. High level expression of CD43 inhibits T cell receptor/CD3-mediated apoptosis. *J Exp Med* 1999; **190**: 1903–1908.
- *285. Delon J, Kaibuchi K, Germain RN. Exclusion of CD43 from the immunological synapse is mediated by phosphorylation-regulated relocation of the cytoskeletal adaptor moesin. *Immunity* 2001; **15**: 691–701.
- *286. Avallé L, Pensa S, Regis G, et al. STAT1 and STAT3 in tumorigenesis: a matter of balance. *JAKSTAT* 2012; **1**: 65–72.
- *287. Koch MA, Tucker-Heard G, Perdue NR, et al. The transcription factor T-bet controls regulatory T cell homeostasis and function during type 1 inflammation. *Nat Immunol* 2009; **10**: 595–602.
- *288. Robertson AG, Shih J, Yau C, et al. Integrative analysis identifies four molecular and clinical subsets in uveal melanoma. *Cancer Cell* 2017; **32**: 204–220.e15.
- *289. Grimmig T, Matthes N, Hoeland K, et al. TLR7 and TLR8 expression increases tumor cell proliferation and promotes chemoresistance in human pancreatic cancer. *Int J Oncol* 2015; **47**: 857–866.
- *290. Chatterjee S, Crozet L, Damotte D, et al. TLR7 promotes tumor progression, chemotherapy resistance, and poor clinical outcomes in non-small cell lung cancer. *Cancer Res* 2014; **74**: 5008–5018.
- *291. Ye J, Ma C, Hsueh EC, et al. TLR8 signaling enhances tumor immunity by preventing tumor-induced T-cell senescence. *EMBO Mol Med* 2014; **6**: 1294–1311.
- *292. Oliver JL, Alexander MP, Norrod AG, et al. Differential expression and tumor necrosis factor-mediated regulation of TNFRSF11b/osteoprotegerin production by human melanomas. *Pigment Cell Melanoma Res* 2013; **26**: 571–579.
- *293. Renema N, Navet B, Heymann MF, et al. RANK–RANKL signaling in cancer. *Biosci Rep* 2016; **36**: e00366.
- *294. Anderson DM, Maraskovsky E, Billingsley WL, et al. A homologue of the TNF receptor and its ligand enhance T-cell growth and dendritic-cell function. *Nature* 1997; **390**: 175–179.
- *295. Vanamee ES, Faustman DL. TNFR2: a novel target for cancer immunotherapy. *Trends Mol Med* 2017; **23**: 1037–1046.
- *296. Zhao Y, Tahiliani V, Salek-Ardakani S, et al. Targeting 4-1BB (CD137) to enhance CD8 T cell responses with poxviruses and viral antigens. *Front Immunol* 2012; **3**: 332.
- *297. Kwon B. Anti-CD137 cancer immunotherapy suppresses tumor growth-response. *Cancer Res* 2018; **78**: 1572–1573.
- *298. Merino D, Lalaoui N, Morizot A, et al. TRAIL in cancer therapy: present and future challenges. *Expert Opin Ther Targets* 2007; **11**: 1299–1314.
- *299. Mackay F, Browning JL. BAFF: a fundamental survival factor for B cells. *Nat Rev Immunol* 2002; **2**: 465–475.
- *300. Mackay F, Leung H. The role of the BAFF/APRIL system on T cell function. *Semin Immunol* 2006; **18**: 284–289.
- *301. Zhang Z, Li LY. TNFSF15 modulates neovascularization and inflammation. *Cancer Microenviron* 2012; **5**: 237–247.
- *302. Lalani AI, Moore CR, Luo C, et al. Myeloid cell TRAF3 regulates immune responses and inhibits inflammation and tumor development in mice. *J Immunol* 2015; **194**: 334–348.
- *303. Paschen A, Sucker A, Hill B, et al. Differential clinical significance of individual NKG2D ligands in melanoma: soluble ULBP2 as an indicator of poor prognosis superior to S100B. *Clin Cancer Res* 2009; **15**: 5208–5215.
- *304. Gasser S, Orsulic S, Brown EJ, et al. The DNA damage pathway regulates innate immune system ligands of the NKG2D receptor. *Nature* 2005; **436**: 1186–1190.
- *305. Au-Yeung BB, Levin SE, Zhang C, et al. A genetically selective inhibitor demonstrates a function for the kinase Zap70 in regulatory T cells independent of its catalytic activity. *Nat Immunol* 2010; **11**: 1085–1092.
- *306. Schmidt AM, Lu W, Sindhava VJ, et al. Regulatory T cells require TCR signaling for their suppressive function. *J Immunol* 2015; **194**: 4362–4370.
- *307. Wang H, Kadlec TA, Au-Yeung BB, et al. ZAP-70: an essential kinase in T-cell signaling. *Cold Spring Harb Perspect Biol* 2010; **2**: a002279.
- *Cited only in supplementary material.

SUPPLEMENTARY MATERIAL ONLINE

Supplementary materials and methods

Supplementary figure legends

Figure S1. Effects of chromosome 3 loss

Figure S2. Immunohistochemistry analysis of one BAP1⁻ mUM for selective immune markers: CD3, CD4, CD8, CD68, CD38, TIA1, and Tbet

Figure S3. Mass cytometry results

Table S1. Immune categories combined from the nCounter PanCancer immune profiling gene set with a literature review

Table S2. Immune categories for supervised network analysis

Table S3. Leukocyte immune response categories

Table S4. Mass cytometry antibodies and reagents

Table S5. Immune genes Spearman's correlation with BAP1 expression or Chr3 loss

Table S6. Spearman's rank correlation coefficient (r) and P values of immune genes exclusively correlated with BAP1 gene expression

Table S7. Spearman's rank correlation coefficient (r) and P values of immune genes with better correlation to BAP1 gene expression than Chr3 copy number variations

Table S8. List of Kaplan–Meier survival test scores and P values in the context of BAP1 loss

Table S9. Spearman's rank correlation coefficient (r) and P values of immune genes that exclusively correlate with Chr3 copy number variations (M3-UM)

Table S10. Spearman's rank correlation coefficient (r) and P values of immune genes with better correlation to Chr3 copy number variations (M3-UM) than BAP1 gene expression

Table S11. List of Kaplan–Meier survival test scores and P values in the context of Chr3 copy number variation